

# Algebraic models of hadron structure: I. Nonstrange baryons

R. Bijker

R.J. Van de Graaff Laboratory, University of Utrecht,  
P.O. Box 80000, 3508 TA Utrecht, The Netherlands

F. Iachello

Center for Theoretical Physics, Sloane Laboratory,  
Yale University, New Haven, CT 06511, U.S.A.

A. Leviatan

Racah Institute of Physics, The Hebrew University,  
Jerusalem 91904, Israel

## Abstract

We introduce an algebraic framework for the description of baryons. Within this framework we study a collective string-like model and show that this model gives a good overall description of the presently available data. We discuss in particular masses and electromagnetic couplings, including the transition form factors that can be measured at new electron facilities.

## 1 Introduction

In the last 20 years QCD has emerged as the theory of strong interactions. This theory has been tested in the perturbative regime by several experiments at CERN and other laboratories. However, in the nonperturbative regime, defined in this article as  $E \lesssim 3$  GeV, no solution of QCD is known, except for lattice calculations of the ground state and its properties. Even with the development of new dedicated computers, the lattice calculation of the excitation spectrum of hadrons is a daunting problem and its solution is still years away.

In a series of papers starting with this one we address the problem of the spectroscopy of baryons in the nonperturbative regime using methods introduced in this field 30 years ago to describe its flavor-spin part [1] and extended here to include the space part. This extension is stimulated by the success that the use of algebraic methods has had in other fields of physics, most notably nuclear [2] and molecular [3] physics. By making use of these methods we are able to calculate in a straightforward way all observable quantities and thus test various models of hadronic structure. In particular, we are able to contrast the nonrelativistic [4] or relativized [5] valence quark models with string-like models. In doing so, we also provide a more transparent understanding of the extent to which the nonrelativistic reduction of the perturbative one-gluon exchange interaction used in [4, 5] holds in the nonperturbative regime. However, the main purpose of this article is not so much that of testing well-known models, but rather that of (i) introducing the algebraic framework and, most importantly, of (ii) studying a new ‘collective’ model of baryons which appears to give a realistic description *vis à vis* the experimental data, especially in the form factors.

The outline of this article is as follows: in Sections 2–4 we present some general properties of the algebraic approach, in Sections 5 and 6 we discuss the mass spectrum and in Sections 7–10 the

electromagnetic couplings of nonstrange baryons. Some of the more technical details are presented in the appendices.

## 2 Models of baryons

We consider baryons to be built of three constituent parts. The global internal quantum numbers of these three parts are taken to be: flavor=triplet=u,d,s; spin=doublet=1/2; and color=triplet (we do not consider here heavy quark flavors). The internal algebraic structure of the constituent parts is thus the usual

$$\mathcal{G}_i = SU_f(3) \otimes SU_s(2) \otimes SU_c(3) . \quad (2.1)$$

(We use in this paper the notation appropriate to groups, *i.e.* upper case letters and  $\otimes$  signs, rather than to algebras, *i.e.* lower case letters and  $\oplus$  signs.) The quantum numbers need not be all concentrated at one point but may be distributed over a volume of size equal to the hadronic size. In particular, in this paper we discuss mostly the string-like configuration depicted in Figure 1. Although the string is fat, we shall, from time to time, idealize it as a thin string with a distribution of mass, charge and magnetic moments. The algebraic method that we shall introduce can easily be applied to the single-particle valence quark model as well and therefore we shall present also results for this model when needed for comparison.

The main purpose of this paper is to study the properties of baryon resonances in terms of a string-like model (see Figure 1), in particular the mass spectrum and electromagnetic couplings. In order to do so, we need a framework within which this study can be done. In the valence quark model this is usually a Schrödinger-like differential equation with two-body interactions. We prefer here instead to use a more general method based on a bosonic quantization of the relevant degrees of freedom. This method has been extensively used in nuclear and molecular physics [6]. The relevant degrees of freedom characterizing the configuration in Figure 1 are the two Jacobi coordinates  $\vec{\rho}$ ,  $\vec{\lambda}$  (in addition to the center-of-mass coordinate which is not relevant for the excitation spectrum). The relative Jacobi coordinates are given by

$$\begin{aligned} \vec{\rho} &= \frac{1}{\sqrt{2}}(\vec{r}_1 - \vec{r}_2) , \\ \vec{\lambda} &= \frac{1}{\sqrt{6}}(\vec{r}_1 + \vec{r}_2 - 2\vec{r}_3) , \end{aligned} \quad (2.2)$$

where  $\vec{r}_1$ ,  $\vec{r}_2$  and  $\vec{r}_3$  denote the end points of the string configuration in Figure 1. The method of bosonic quantization consists in introducing two vector boson operators (one for each relative coordinate) which are related to the coordinates,  $\vec{\rho}$  and  $\vec{\lambda}$ , and their conjugate momenta,  $\vec{p}_\rho$  and  $\vec{p}_\lambda$ , by

$$\begin{aligned} b_{\rho,m}^\dagger &= \frac{1}{\sqrt{2}}(\rho_m - i p_{\rho,m}) , \\ b_{\rho,m} &= \frac{1}{\sqrt{2}}(\rho_m + i p_{\rho,m}) , \\ b_{\lambda,m}^\dagger &= \frac{1}{\sqrt{2}}(\lambda_m - i p_{\lambda,m}) , \\ b_{\lambda,m} &= \frac{1}{\sqrt{2}}(\lambda_m + i p_{\lambda,m}) , \end{aligned} \quad (2.3)$$

with  $m = -1, 0, 1$ , and an additional auxiliary scalar boson,  $s^\dagger$ ,  $s$ . These operators satisfy usual boson commutation relations and operators of different type commute. If we denote generically the set of seven creation operators by  $c_\alpha^\dagger$ ,

$$b_{\rho,m}^\dagger , b_{\lambda,m}^\dagger , s^\dagger \equiv c_\alpha^\dagger , \quad (2.4)$$

with  $\alpha = 1, \dots, 7$ , the bilinear products

$$\mathcal{G}_r : G_{\alpha\alpha'} = c_\alpha^\dagger c_{\alpha'} , \quad (2.5)$$

with  $\alpha, \alpha' = 1, \dots, 7$  generate the Lie algebra of  $U(7)$ . This bosonic quantization scheme follows the usual prescription that any problem in  $\nu$  space degrees of freedom be written in terms of elements of the Lie algebra  $U(\nu + 1)$ , and that all its states be assigned to the totally symmetric representation  $[N]$  of  $U(\nu + 1)$  [7]. All operators can be expanded into elements of  $\mathcal{G}_r = U(7)$ , and states can be constructed by acting with the boson operators on a vacuum

$$\frac{1}{\mathcal{N}} (b_\rho^\dagger)^{n_\rho} (b_\lambda^\dagger)^{n_\lambda} (s^\dagger)^{N-n_\rho-n_\lambda} |0\rangle , \quad (2.6)$$

where  $\mathcal{N}$  is a normalization factor. The complete algebraic structure of the problem is thus

$$\mathcal{G} = \mathcal{G}_r \otimes \mathcal{G}_i = U(7) \otimes SU_f(3) \otimes SU_s(2) \otimes SU_c(3) . \quad (2.7)$$

$\mathcal{G}$  is the spectrum generating algebra (SGA) of baryon structure.

### 3 The algebra of $U(7)$

We want to construct states and operators that transform according to irreducible representations of the rotation group (since the problem is rotationally invariant). The creation operators,  $b_\rho^\dagger$  and  $b_\lambda^\dagger$ , transform by definition as vectors under rotation. The annihilation operators do not. It is easy to construct operators that transform appropriately. They are

$$\begin{aligned} \tilde{b}_{\rho,m} &= (-1)^{1-m} b_{\rho,-m} , \\ \tilde{b}_{\lambda,m} &= (-1)^{1-m} b_{\lambda,-m} , \\ \tilde{s} &= s . \end{aligned} \quad (3.1)$$

Using these operators one can rewrite the 49 elements of  $U(7)$  in their angular-momentum coupled Racah form

$$(c_l^\dagger \times \tilde{c}_{l'})_M^{(L)} = \sum_{m,m'} \langle l, m, l', m' | L, M \rangle c_{l,m}^\dagger \tilde{c}_{l',m'} , \quad (3.2)$$

where  $c_l^\dagger$  ( $\tilde{c}_l$ ) for  $l = 1$  denotes the vector bosons  $b_\rho^\dagger$  ( $\tilde{b}_\rho$ ),  $b_\lambda^\dagger$  ( $\tilde{b}_\lambda$ ) and for  $l = 0$  the scalar boson  $s^\dagger$  ( $\tilde{s}$ ). The cross denotes a tensor product with respect to  $SO(3)$ .

Another unavoidable problem in baryon structure is that, if some of the constituent parts are identical, one must construct states and operators that transform according to representations of the permutation group (either  $S_3$  for three identical parts or  $S_2$  for two identical parts). The problem is particularly acute for nonstrange baryons, if one assumes that the three constituent parts are identical. In this case one must construct operators that transform as irreducible representations of  $S_3$ . In this construction [8], we use the transposition  $P(12)$  and the cyclic permutation  $P(123)$ . All other permutations can be expressed in terms of these two elementary ones. The transformation properties under  $S_3$  of all operators of interest follow from those of the building blocks. Using the definitions of Eqs. (2.2) and (2.3), one has the following transformation properties of the creation operators under  $S_3$

$$\begin{aligned} P(12) \begin{pmatrix} s^\dagger \\ b_{\rho,m}^\dagger \\ b_{\lambda,m}^\dagger \end{pmatrix} &= \begin{pmatrix} 1 & 0 & 0 \\ 0 & -1 & 0 \\ 0 & 0 & 1 \end{pmatrix} \begin{pmatrix} s^\dagger \\ b_{\rho,m}^\dagger \\ b_{\lambda,m}^\dagger \end{pmatrix} , \\ P(123) \begin{pmatrix} s^\dagger \\ b_{\rho,m}^\dagger \\ b_{\lambda,m}^\dagger \end{pmatrix} &= \begin{pmatrix} 1 & 0 & 0 \\ 0 & \cos(2\pi/3) & \sin(2\pi/3) \\ 0 & -\sin(2\pi/3) & \cos(2\pi/3) \end{pmatrix} \begin{pmatrix} s^\dagger \\ b_{\rho,m}^\dagger \\ b_{\lambda,m}^\dagger \end{pmatrix} . \end{aligned} \quad (3.3)$$

There are three different symmetry classes for the permutation of three objects:

$$\begin{aligned}
\Box\Box\Box &\equiv S(\text{ymmetric}) \\
\Box\Box &\equiv M(\text{ixed symmetry}) \\
\Box &\equiv A(\text{ntisymmetric})
\end{aligned} \tag{3.4}$$

with dimensions 1, 2 and 1, respectively. Eq. (3.3) shows that the scalar boson,  $s^\dagger$ , transforms as the symmetric representation,  $S$ , while the two vector bosons,  $b_\rho^\dagger$  and  $b_\lambda^\dagger$ , transform as the two components,  $M_\rho$  and  $M_\lambda$ , of the mixed symmetry representation. Alternatively, the three symmetry classes can be labeled by the irreducible representations of the point group  $D_3$  (which is isomorphic to  $S_3$ ) as  $A_1$ ,  $E$  and  $A_2$ , respectively.

Now we can rewrite the 49 elements of the algebra of  $U(7)$  in terms of the operators that transform as irreducible representations of  $SO(3)$  and  $S_3$ ,

$$\begin{aligned}
\hat{D}_{\rho,m} &= (b_\rho^\dagger \times \tilde{s} - s^\dagger \times \tilde{b}_\rho)_m^{(1)} , \\
\hat{D}_{\lambda,m} &= (b_\lambda^\dagger \times \tilde{s} - s^\dagger \times \tilde{b}_\lambda)_m^{(1)} , \\
\hat{A}_{\rho,m} &= i(b_\rho^\dagger \times \tilde{s} + s^\dagger \times \tilde{b}_\rho)_m^{(1)} , \\
\hat{A}_{\lambda,m} &= i(b_\lambda^\dagger \times \tilde{s} + s^\dagger \times \tilde{b}_\lambda)_m^{(1)} , \\
\hat{G}_{M_\rho,m}^{(l)} &= (b_\rho^\dagger \times \tilde{b}_\lambda + b_\lambda^\dagger \times \tilde{b}_\rho)_m^{(l)} , \\
\hat{G}_{M_\lambda,m}^{(l)} &= (b_\rho^\dagger \times \tilde{b}_\rho - b_\lambda^\dagger \times \tilde{b}_\lambda)_m^{(l)} , \\
\hat{G}_{S,m}^{(l)} &= (b_\rho^\dagger \times \tilde{b}_\rho + b_\lambda^\dagger \times \tilde{b}_\lambda)_m^{(l)} , \\
\hat{G}_{A,m}^{(l)} &= i(b_\rho^\dagger \times \tilde{b}_\lambda - b_\lambda^\dagger \times \tilde{b}_\rho)_m^{(l)} , \\
\hat{n}_s &= (s^\dagger \times \tilde{s})_0^{(0)} ,
\end{aligned} \tag{3.5}$$

with  $l = 0, 1, 2$ . For future reference, we present here the explicit expressions of some other operators of interest. They are all linear combinations of the generators of Eq. (3.5)

$$\begin{aligned}
\hat{n}_\rho &= \sqrt{3}(b_\rho^\dagger \times \tilde{b}_\rho)_0^{(0)} , \\
\hat{n}_\lambda &= \sqrt{3}(b_\lambda^\dagger \times \tilde{b}_\lambda)_0^{(0)} , \\
\hat{N} &= \hat{n}_s + \hat{n}_\rho + \hat{n}_\lambda , \\
\hat{L}_m &= \sqrt{2}\hat{G}_{S,m}^{(1)} , \\
\hat{K}_y &= -\sqrt{3}\hat{G}_{A,0}^{(0)} .
\end{aligned} \tag{3.6}$$

Also for future reference and in view of the fact that this problem is of relevance to other fields as well (triatomic molecules [9]), we summarize in Table I the transformation properties of some linear and bilinear combinations of boson operators.

## 4 Basis states

In order to do calculations one needs to construct a complete set of basis states for the representations of  $U(7)$ . These are obtained by considering subalgebras of  $U(7)$ . There are two bases of

particular interest:

$$U(7) \supset U_\rho(3) \otimes U_\lambda(4) \supset \left\{ \begin{array}{l} U_\rho(3) \otimes U_\lambda(3) \\ U_\rho(3) \otimes SO_\lambda(4) \end{array} \right\} \supset SO_\rho(3) \otimes SO_\lambda(3) \supset SO(3) \supset SO(2) . \quad (4.1)$$

The first one corresponds to two coupled three-dimensional harmonic oscillators. The states in this basis are characterized by a set of quantum numbers related to the irreducible representations of the subgroups

$$\left| \begin{array}{ccccccc} U(7) & \supset & U_\rho(3) & \otimes & U_\lambda(4) & \supset & U_\rho(3) & \otimes & U_\lambda(3) \\ \downarrow & & \downarrow & & & & \downarrow & & \downarrow \\ N & & n_\rho & & & & n_\lambda & & \\ & & & \supset & SO_\rho(3) & \otimes & SO_\lambda(3) & \supset & SO(3) & \supset & SO(2) \\ & & & & \downarrow & & \downarrow & & \downarrow & & \downarrow \\ & & & & L_\rho & & L_\lambda & & L & & M_L \end{array} \right\} . \quad (4.2)$$

For a given value of  $N$ , *i.e.* the model space in which calculations are done, one has

$$\begin{aligned} n_\rho &= 0, 1, \dots, N , \\ n_\lambda &= 0, 1, \dots, N - n_\rho , \\ L_\rho &= n_\rho, n_\rho - 2, \dots, 1 \text{ or } 0 , \\ L_\lambda &= n_\lambda, n_\lambda - 2, \dots, 1 \text{ or } 0 , \\ L &= |L_\rho - L_\lambda|, |L_\rho - L_\lambda| + 1, \dots, L_\rho + L_\lambda , \\ M_L &= -L, -L + 1, \dots, L . \end{aligned} \quad (4.3)$$

The parity of the state is  $\pi = (-)^{L_\rho + L_\lambda}$ . The basis states are then uniquely labeled by

$$|N, (n_\rho, L_\rho), (n_\lambda, L_\lambda); L, M_L\rangle . \quad (4.4)$$

The same basis of two coupled harmonic oscillators is employed in the nonrelativistic and relativized quark models. Early quark model calculations [4] used  $n_\rho + n_\lambda \leq 2$ , while more recent calculations [5] have used  $n_\rho + n_\lambda \leq 6$ . These choices correspond in  $U(7)$  to taking the total number of bosons equal to  $N = 2$  and  $N = 6$ , respectively.

The second basis is very convenient to evaluate matrix elements of the electromagnetic transition operator (see Appendix D). It corresponds to a coupled system of a three-dimensional harmonic oscillator,  $U_\rho(3)$ , and a three-dimensional Morse oscillator,  $SO_\lambda(4)$ . The states in this basis are labeled by

$$\left| \begin{array}{ccccccc} U(7) & \supset & U_\rho(3) & \otimes & U_\lambda(4) & \supset & U_\rho(3) & \otimes & SO_\lambda(4) \\ \downarrow & & \downarrow & & & & \downarrow & & \downarrow \\ N & & n_\rho & & & & \omega & & \\ & & & \supset & SO_\rho(3) & \otimes & SO_\lambda(3) & \supset & SO(3) & \supset & SO(2) \\ & & & & \downarrow & & \downarrow & & \downarrow & & \downarrow \\ & & & & L_\rho & & L_\lambda & & L & & M_L \end{array} \right\} . \quad (4.5)$$

For a given value of  $N$  the allowed values of the quantum numbers are given by

$$\begin{aligned} \omega &= N - n_\rho, N - n_\rho - 2, \dots, 1 \text{ or } 0 , \\ L_\lambda &= 0, 1, \dots, \omega . \end{aligned} \quad (4.6)$$

The allowed values of  $n_\rho$ ,  $L_\rho$ ,  $L$  and  $M_L$  are the same as in the harmonic oscillator basis. The parity is  $\pi = (-)^{L_\rho + L_\lambda}$ . Summarizing, the basis states are uniquely labeled by

$$|N, (n_\rho, L_\rho), (\omega, L_\lambda); L, M_L\rangle . \quad (4.7)$$

## 5 Mass operator

In general the mass operator depends both on the spatial and the internal degrees of freedom. We first discuss the contribution from the spatial part and then that of the spin-flavor part.

### 5.1 Space part

The algebraic framework of the previous sections allows one to study the excitation spectra of objects with the geometric shape of Figure 1. In nonrelativistic problems the spectrum is obtained by expanding the hamiltonian in terms of operators of the algebra  $\mathcal{G}_r$ . Here we prefer to expand the mass-squared operator into elements of  $\mathcal{G}_r$ ,

$$\hat{M}^2 = f(G_{\alpha\alpha'}), \quad G_{\alpha\alpha'} \in \mathcal{G}_r. \quad (5.1)$$

The expansion is usually a polynomial in  $G_{\alpha\alpha'}$ . When the three constituent parts are identical, the mass-squared operator must transform as the symmetric representation  $S$  (or  $A_1$ ) of  $S_3$  (or  $D_3$ ). The most general  $\hat{M}^2$  operator that preserves angular momentum and parity, transforms as a scalar under the permutation group, and is at most quadratic in  $G_{\alpha\alpha'}$  is

$$\begin{aligned} \hat{M}^2 = & M_0^2 + \epsilon_s s^\dagger \tilde{s} - \epsilon_p (b_\rho^\dagger \cdot \tilde{b}_\rho + b_\lambda^\dagger \cdot \tilde{b}_\lambda) + u_0 (s^\dagger s^\dagger \tilde{s} \tilde{s}) - u_1 s^\dagger (b_\rho^\dagger \cdot \tilde{b}_\rho + b_\lambda^\dagger \cdot \tilde{b}_\lambda) \tilde{s} \\ & + v_0 \left[ (b_\rho^\dagger \cdot b_\rho^\dagger + b_\lambda^\dagger \cdot b_\lambda^\dagger) \tilde{s} \tilde{s} + s^\dagger s^\dagger (\tilde{b}_\rho \cdot \tilde{b}_\rho + \tilde{b}_\lambda \cdot \tilde{b}_\lambda) \right] \\ & + \sum_{l=0,2} c_l \left[ (b_\rho^\dagger \times b_\rho^\dagger - b_\lambda^\dagger \times b_\lambda^\dagger)^{(l)} \cdot (\tilde{b}_\rho \times \tilde{b}_\rho - \tilde{b}_\lambda \times \tilde{b}_\lambda)^{(l)} + 4 (b_\rho^\dagger \times b_\lambda^\dagger)^{(l)} \cdot (\tilde{b}_\lambda \times \tilde{b}_\rho)^{(l)} \right] \\ & + c_1 (b_\rho^\dagger \times b_\lambda^\dagger)^{(1)} \cdot (\tilde{b}_\lambda \times \tilde{b}_\rho)^{(1)} + \sum_{l=0,2} w_l (b_\rho^\dagger \times b_\rho^\dagger + b_\lambda^\dagger \times b_\lambda^\dagger)^{(l)} \cdot (\tilde{b}_\rho \times \tilde{b}_\rho + \tilde{b}_\lambda \times \tilde{b}_\lambda)^{(l)}. \end{aligned} \quad (5.2)$$

Here the dots indicate scalar products and the crosses tensor products as usual. If the three objects are not identical (as is the case in strange baryons) or if the interactions between the three objects are not identical (as is the case if there is a flavor-spin dependence), the mass-squared operator is no longer invariant under  $S_3$ , and a more general form, still within  $U(7)$ , arises. This situation will be discussed in a subsequent publication.

The eigenvalues and corresponding eigenvectors of the mass-squared operator in Eq. (5.2) can be obtained exactly by diagonalization in the basis of either Eq. (4.4) or (4.7). In Appendix A we describe how the matrix elements in either basis are calculated. The wave functions obtained in this way have by construction good angular momentum, parity and permutation symmetry. The permutation symmetry of a given wave function is determined as follows. Firstly, since Eq. (5.2) is invariant under the transposition  $P(12)$ , basis states with  $n_\rho$  even and  $n_\rho$  odd do not mix, and can therefore be treated separately. This allows one to distinguish between states with  $S, M_\lambda$  and states with  $A, M_\rho$  symmetry. Secondly, we note that the operator  $\hat{K}_y^2$  (where  $\hat{K}_y$  is given in Eq. (3.6)) commutes with the  $S_3$ -invariant mass-squared operator of Eq. (5.2) and has expectation values,  $K_y^2$  (with  $K_y = 0, \pm 1, \pm 2, \dots$ ). Since the cyclic permutation  $P(123)$  acts in Fock space as a rotation of  $\theta = 2\pi/3$  induced by  $\hat{K}_y$ :  $\exp[-i\theta\hat{K}_y]$ , one finds that for  $|K_y| = 0 \pmod{3}$  the wave functions transform as  $S$  or  $A$ , whereas for  $|K_y| = 1, 2 \pmod{3}$  they transform as  $M_\rho$  or  $M_\lambda$ . In conclusion, the transposition separates  $S, M_\lambda$  from  $A, M_\rho$  and the cyclic permutation separates  $S, A$  from  $M_\rho, M_\lambda$ . We note that the quantum number  $K_y$  is analogous to the label  $m$  used in [11], since the operator  $\hat{n}_\zeta - \hat{n}_\eta$  of [11] is equal to  $\hat{K}_y$ .

Eq. (5.2) contains several models of baryon structure. These models correspond to different choices of the coefficients in Eq. (5.2). We mention in particular two classes of models:

(i) Single-particle (harmonic oscillator) quark models. These correspond to the choice  $v_0 = 0$ , *i.e.* no coupling between different harmonic oscillator shells,

$$\hat{M}^2 = M_0^2 + \epsilon_s s^\dagger s - \epsilon_p (b_\rho^\dagger \cdot \tilde{b}_\rho + b_\lambda^\dagger \cdot \tilde{b}_\lambda) + \text{anharmonic terms}, \quad (5.3)$$

or, introducing the number operators of Eq. (3.6)

$$\hat{M}^2 = M_0^2 + \epsilon_s \hat{N} + (\epsilon_\rho - \epsilon_s) (\hat{n}_\rho + \hat{n}_\lambda) + \text{anharmonic terms} . \quad (5.4)$$

The nonrelativistic harmonic oscillator quark model [4] is a model of this type, although it is written for the mass  $\hat{M}$  rather than for  $\hat{M}^2$ ,

$$\begin{aligned} \hat{M} &= \frac{p_\rho^2}{2\mu} + \frac{p_\lambda^2}{2\mu} + \frac{3}{2}\kappa\rho^2 + \frac{3}{2}\kappa\lambda^2 + \text{perturbations} \\ &= \epsilon(-b_\rho^\dagger \cdot \tilde{b}_\rho - b_\lambda^\dagger \cdot \tilde{b}_\lambda + 3) + \text{perturbations} \\ &= \epsilon(\hat{n}_\rho + \hat{n}_\lambda + 3) + \text{perturbations} , \end{aligned} \quad (5.5)$$

with  $\epsilon = \sqrt{3\kappa/\mu}$ . The perturbations involve both anharmonic terms and terms that couple different shells, but the breaking is relatively small. For example, the nucleon wave function in these type of models is still dominated by the  $n_\rho + n_\lambda = 0$  component (typically of the order 80% [12]). The unperturbed harmonic oscillator quark model corresponds algebraically to the decomposition of  $U(7)$  into  $U(6) \otimes U(1)$ . All results of these models are contained in  $U(7)$ , provided that the expansion in terms of elements  $G_{\alpha\alpha'}$  is made for the mass operator rather than its square. In Figure 2 we show the spectrum for the unperturbed harmonic oscillator.

(ii) Collective (string) models. In these models the three constituent parts move in a correlated way. They correspond to the choice  $v_0 \neq 0$ . Since in this case the mass-squared operator contains terms of the type  $b^\dagger b^\dagger s s + s^\dagger s^\dagger b b$ , the corresponding eigenfunctions are spread over many oscillator shells. In order to study models of this type (which is the main and novel purpose of this paper), it is instructive to rewrite the mass-squared operator of Eq. (5.2) in terms of vibrational and rotational contributions to the mass spectrum. The general procedure for such a decomposition was introduced [13] for the Interacting Boson Model in nuclear physics. Here we apply the same method to the  $S_3$ -invariant mass operator of Eq. (5.2) [8]

$$\hat{M}^2 = \hat{M}_0^2 + \hat{M}_{\text{vib}}^2 + \hat{M}_{\text{rot}}^2 + \hat{M}_{\text{vib-rot}}^2 , \quad (5.6)$$

with

$$\begin{aligned} \hat{M}_{\text{vib}}^2 &= \xi_1 \left( R^2 s^\dagger s^\dagger - b_\rho^\dagger \cdot b_\rho^\dagger - b_\lambda^\dagger \cdot b_\lambda^\dagger \right) \left( R^2 \tilde{s}\tilde{s} - \tilde{b}_\rho \cdot \tilde{b}_\rho - \tilde{b}_\lambda \cdot \tilde{b}_\lambda \right) \\ &\quad + \xi_2 \left[ \left( b_\rho^\dagger \cdot b_\rho^\dagger - b_\lambda^\dagger \cdot b_\lambda^\dagger \right) \left( \tilde{b}_\rho \cdot \tilde{b}_\rho - \tilde{b}_\lambda \cdot \tilde{b}_\lambda \right) + 4 \left( b_\rho^\dagger \cdot b_\lambda^\dagger \right) \left( \tilde{b}_\lambda \cdot \tilde{b}_\rho \right) \right] , \\ \hat{M}_{\text{rot}}^2 &= 2\xi_3 \hat{G}_S^{(1)} \cdot \hat{G}_S^{(1)} + 3\xi_4 \hat{G}_A^{(0)} \cdot \hat{G}_A^{(0)} \\ &= \xi_3 \hat{L} \cdot \hat{L} + \xi_4 \hat{K}_y \cdot \hat{K}_y , \\ \hat{M}_{\text{vib-rot}}^2 &= \xi_5 \left[ \hat{A}_\rho \cdot \hat{A}_\rho + \hat{A}_\lambda \cdot \hat{A}_\lambda \right] + \xi_6 \left[ \hat{G}_{M_\rho}^{(1)} \cdot \hat{G}_{M_\rho}^{(1)} + \hat{G}_{M_\lambda}^{(1)} \cdot \hat{G}_{M_\lambda}^{(1)} \right] , \\ \hat{M}_0^2 &= \xi_7 + \xi_8 (\hat{n}_\rho + \hat{n}_\lambda) . \end{aligned} \quad (5.7)$$

The explicit expression of  $\hat{G}_S^{(1)}, \dots$ , in terms of boson operators is given in Eqs. (3.5) and (3.6). By rewriting  $\hat{M}^2$  in this form one emphasizes the physical content of the string-like model, since the excitation spectrum will now appear as vibrations and rotations of the string-like configuration shown in Figure 1. The new parameters in Eq. (5.7) are linear combinations of those in Eq. (5.2).

Although the mass spectrum and corresponding eigenfunctions of  $\hat{M}^2$  can be obtained numerically by diagonalization, we prefer here to use coherent states to gain further insight into the physical content of each contribution. To this end, we use the coherent (or intrinsic) states of Appendix B. We begin by considering the vibrational term  $\hat{M}_{\text{vib}}^2$ . The Bose condensate of Eq. (B.2) is the lowest eigenstate of this term ( $\xi_1, \xi_2 > 0$ ). Indeed the separation (5.6) has been done in order to satisfy this condition. For large  $N$  higher eigenstates are of the type (B.4) and, to leading order in  $N$ , the corresponding eigenvalues are given by [8]

$$M_{\text{vib}}^2 = N [\kappa_1 n_u + \kappa_2 (n_v + n_w)] , \quad (5.8)$$

where  $n_u, n_v, n_w (\geq 0)$  are the eigenvalues of the number operators  $b_u^\dagger b_u, b_v^\dagger b_v, b_w^\dagger b_w$  (the  $b_u^\dagger, b_v^\dagger, b_w^\dagger$  operators are given in Eq. (B.1)), and

$$\begin{aligned}\kappa_1 &= 4 \xi_1 R^2, \\ \kappa_2 &= 4 \xi_2 R^2 (1 + R^2)^{-1}.\end{aligned}\tag{5.9}$$

The vibrational part of the mass-squared operator of Eq. (5.6) has a very simple physical interpretation. Its spectrum has three fundamental vibrations (see Figure 3). The  $u$ -vibration is the symmetric stretching vibration along the direction of the strings (breathing mode), while the  $v$ - and the  $w$ -vibrations denote bending vibrations of the strings. The latter two vibrations are degenerate in the case of three identical objects [14]. We note in passing that QCD based arguments suggest that while the string is soft towards stretching, it is hard towards bending and thus one expects the  $v$ - and  $w$ -vibrations to lie higher than the  $u$ -vibration.

Next we discuss the rotational part of the mass-squared operator. It contains two terms that commute with the general  $S_3$ -invariant mass operator of Eq. (5.2) and hence correspond to exact symmetries. The eigenvalues of these rotational terms are

$$M_{\text{rot}}^2 = \xi_3 L(L+1) + \xi_4 K_y^2.\tag{5.10}$$

Here  $L$  is the orbital angular momentum and  $K_y$  corresponds in the large  $N$  limit to the projection  $K$  of the angular momentum on the threefold symmetry axis (the  $y$ -axis in Figure 15). For the ground state band the values of  $L$  and  $K_y$  are

$$\begin{aligned}L &= 0, 1, 2, \dots, L_{\text{max}}, \\ K_y &= 0, \pm 1, \dots, \pm L.\end{aligned}\tag{5.11}$$

For the excited bands the situation is slightly more complicated and it will not be discussed here. Again the physical interpretation of Eq. (5.10) is simple, since it describes the rotational spectrum of the string-like configuration of Figure 1. For finite  $N$  the rotational spectrum is truncated at a finite value of  $L = L_{\text{max}}$ , while for  $N \rightarrow \infty$  also  $L_{\text{max}} \rightarrow \infty$ .

The discussion up to this point applies to any object with the geometric configuration of Figure 1. However, the rotational spectrum of Eq. (5.10) does not reproduce a characteristic feature of hadronic spectra (expected on the basis of QCD [15] and investigated decades ago), namely, the occurrence of linear Regge trajectories. But, since  $L$  and  $K_y$  are good quantum numbers one can consider, still remaining within  $U(7)$ , more complicated functional forms,  $f(\hat{L}^2) + g(\hat{K}_y^2)$ , with eigenvalues,  $f(L(L+1)) + g(K_y^2)$ . Linear Regge trajectories are simply obtained by choosing the form

$$\hat{M}_{\text{rot}}^2 = \alpha \sqrt{\hat{L} \cdot \hat{L} + 1/4} + \beta \sqrt{\hat{K}_y \cdot \hat{K}_y},\tag{5.12}$$

with eigenvalues

$$M_{\text{rot}}^2 = \alpha (L + 1/2) + \beta |K_y|.\tag{5.13}$$

The rotational spectrum of Eq. (5.10) and (5.13) is that of an oblate top [14]. If  $\xi_4 = 0$  (or  $\beta = 0$ ) the top is symmetric. When viewed as a top, the configuration of Figure 1 has  $D_3$  point group symmetry. Since  $D_3$  is isomorphic to  $S_3$ , one can label the states either with  $S, M$  and  $A$ , or with the equivalent labels of  $D_3$ , *i.e.*  $A_1, E$  and  $A_2$ ,

$$S \leftrightarrow A_1, \quad M \leftrightarrow E, \quad A \leftrightarrow A_2.\tag{5.14}$$

Unlike the rotational part, the last term in the  $S_3$ -invariant mass-squared operator of Eq. (5.6) does not commute with the vibrational part and hence introduces vibration-rotation interactions. We shall not discuss this term any further, since the experimental mass spectrum of baryons is



not known accurately enough to be able to detect rotation-vibration couplings. Finally, the  $\hat{M}_0^2$  term in Eq. (5.6) contains an overall constant that does not contribute to mass splittings and a one-body term whose contribution is negligible in the large  $N$  limit.

We summarize the results of the present analysis by showing in Figure 4 the spectrum of the string-like configuration of Figure 1, given by the simplified mass formula

$$M^2 = M_0^2 + N [\kappa_1 n_u + \kappa_2 (n_v + n_w)] + \alpha L . \quad (5.15)$$

Here we have discarded the  $K_y$ -dependent term in the rotational part, since the experimental mass spectrum of nonstrange baryons does not provide any compelling evidence for its presence. In Figure 4 we have used the projection  $K$  of the angular momentum (equal to the algebraic  $K_y$  for the ground and first excited vibrational band). All constant contributions have been absorbed into  $M_0^2$ . A comparison with the mass spectrum of the harmonic oscillator in Figure 2 shows that whereas for the harmonic oscillator the excited  $L^\pi = 0^+$  states belong to the two-phonon ( $n = n_\rho + n_\lambda = 2$ ) multiplet, in the collective string model they correspond to one-phonon vibrational excitations and are the bandheads of these fundamental vibrations.

## 5.2 Spin-flavor part

In the previous subsection we have discussed the space part of the mass-squared operator with  $S_3$  symmetry. We turn now to a discussion of the internal degrees of freedom of the constituent parts and construct the corresponding contribution to the mass-squared operator and their eigenfunctions. The spatial part of the baryon wave function, which is determined by the  $U(7)$  mass-squared operator, has to be combined with the spin-flavor and color part, in such a way that the total wave function is antisymmetric

$$|\psi\rangle = |\psi_L\rangle \otimes |\psi_{sf}\rangle \otimes |\psi_c\rangle . \quad (5.16)$$

Here  $|\psi_L\rangle$  denotes the space part,  $|\psi_{sf}\rangle$  the spin-flavor part and  $|\psi_c\rangle$  the color part. Since the color part of the wave function is totally antisymmetric (color singlet), the remaining part (space plus spin-flavor) must be totally symmetric. This implies, for the case of three identical constituent parts (discussed here), that the symmetry of  $|\psi_L\rangle$  under  $S_3$  is the same as the symmetry of  $|\psi_{sf}\rangle$ . The construction of spin-flavor wave functions with good  $S_3$  symmetry is well-known (see, for example, Refs. [4, 16, 17]) and in Appendix C we list the conventions used. We denote the basis states for the spin-flavor part by

$$\left| \begin{array}{cccccc} SU_{sf}(6) & \supset & SU_f(3) & \otimes & SU_s(2) & \supset & SU_I(2) & \otimes & U_Y(1) & \otimes & SO_s(2) \\ \downarrow & & \downarrow & & \downarrow & & \downarrow & & \downarrow & & \downarrow \\ [f_1, f_2, \dots, f_5] & & [\mu_1, \mu_2] & & S & & I & & Y & & M_S \end{array} \right\rangle . \quad (5.17)$$

Here  $S$  denotes the spin,  $I$  the isospin and  $Y$  the hypercharge. An unfortunate (but standard) notation is to label representations not by their Young tableaux but by their dimension. For example, for  $SU_f(3)$ ,

$$\dim[\mu_1, \mu_2] = \frac{1}{2}(\mu_1 + 2)(\mu_2 + 1)(\mu_1 - \mu_2 + 1) , \quad (5.18)$$

which gives 8 for  $[\mu_1, \mu_2] = [2, 1]$  and 10 for  $[3, 0]$ . In the following sections we adopt the standard notation in order to facilitate the comparison with other model calculations. Thus, for example,

$$\left| [3, 0, 0, 0, 0], [2, 1], S = \frac{1}{2}, I = \frac{1}{2}, Y = 1 \right\rangle \equiv |[56], {}^2 8, N\rangle , \quad (5.19)$$

represents the spin-flavor part of the wave function of the ground state of the nucleon. The decomposition of representations of  $SU_{sf}(6)$  into those of  $SU_f(3) \otimes SU_s(2)$  is the standard one

$$[56] \supset {}^2 8 \oplus {}^4 10 ,$$

$$\begin{aligned}
[70] &\supset 2^8 \oplus 4^8 \oplus 2^10 \oplus 2^1 , \\
[20] &\supset 2^8 \oplus 4^1 .
\end{aligned} \tag{5.20}$$

The spin-flavor contribution to the mass-squared operator can be expressed in terms of the generators of the spin-flavor algebra. We consider here only its diagonal part which we write in the Gürsey-Radicati [18] form

$$\begin{aligned}
\hat{M}_{sf}^2 &= a \left[ \hat{C}_2(SU_{sf}(6)) - 45 \right] + b \left[ \hat{C}_2(SU_f(3)) - 9 \right] + b' \left[ \hat{C}_2(SU_I(2)) - \frac{3}{4} \right] \\
&\quad + b'' \left[ \hat{C}_1(U_Y(1)) - 1 \right] + b''' \left[ \hat{C}_2(U_Y(1)) - 1 \right] + c \left[ \hat{C}_2(SU_s(2)) - \frac{3}{4} \right] .
\end{aligned} \tag{5.21}$$

We have defined the operators such that each of the terms vanishes for the ground state of the nucleon (see Eq. (5.19)). The eigenvalues of the Casimir operators in the basis states of Eq. (5.17) are

$$\begin{aligned}
\langle \hat{C}_2(SU_{sf}(6)) \rangle &= \begin{cases} 45 & \text{for } 56 \leftrightarrow A_1 \leftrightarrow S \\ 33 & \text{for } 70 \leftrightarrow E \leftrightarrow M \\ 21 & \text{for } 20 \leftrightarrow A_2 \leftrightarrow A \end{cases} , \\
\langle \hat{C}_2(SU_f(3)) \rangle &= \begin{cases} 9 & \text{for } 8 \\ 18 & \text{for } 10 \\ 0 & \text{for } 1 \end{cases} , \\
\langle \hat{C}_2(SU_I(2)) \rangle &= I(I+1) , \\
\langle \hat{C}_1(U_Y(1)) \rangle &= Y , \\
\langle \hat{C}_2(U_Y(1)) \rangle &= Y^2 , \\
\langle \hat{C}_2(SU_s(2)) \rangle &= S(S+1) .
\end{aligned} \tag{5.22}$$

For nonstrange baryons  $Y = 1$  and the  $b''$  and  $b'''$  terms are not needed. Also the  $b$  and  $b'$  terms can be grouped into a single term. Thus, for the analysis of nonstrange baryons we make use of a simplified form

$$\hat{M}_{sf}^2 = a \left[ \hat{C}_2(SU_{sf}(6)) - 45 \right] + b \left[ \hat{C}_2(SU_f(3)) - 9 \right] + c \left[ \hat{C}_2(SU_s(2)) - \frac{3}{4} \right] . \tag{5.23}$$

with three parameters. The meaning of the three terms is obvious. The spin term represents spin-spin interactions, the flavor term denotes the flavor dependence of the interactions, and the  $SU_{sf}(6)$  term, which according to Eq. (5.22) depends on the permutation symmetry of the wave functions, represents 'signature dependent' interactions. These signature dependent (or exchange) interactions were extensively investigated years ago within the framework of Regge theory [19]. We note in passing that in the usual nonrelativistic and relativized quark models the spin-flavor dependence arises from (i) the constituent quark masses producing a dependence similar to that of the  $b''$  term and (ii) from spin-spin forces  $\vec{\sigma}_i \cdot \vec{\sigma}_j$ , that arise from the contact term of the hyperfine interaction, producing a dependence of the type  $cS(S+1)$ . In this sense, Eq. (5.23) is more general than the corresponding spin-flavor dependence in the quark model.

Finally, there could be terms in the mass-squared operator involving simultaneously both internal and spatial degrees of freedom, *i.e.* of the type

$$\hat{M}^2 = f(G_{\alpha\alpha'}) g(G_i) , \quad G_{\alpha\alpha'} \in \mathcal{G}_r , \quad G_i \in \mathcal{G}_i . \tag{5.24}$$

Among these, we mention: (i) spin-orbit-like interactions

$$\hat{M}_{\text{SO}}^2 = d(\vec{S} \cdot \vec{L}) , \tag{5.25}$$

and (ii) tensor-like interactions

$$\hat{M}_{\text{tensor}}^2 = d'(\hat{T}_S^{(2)} \cdot \hat{T}_L^{(2)}) , \tag{5.26}$$

where  $\hat{T}_S^{(2)}$  and  $\hat{T}_L^{(2)}$  are tensors of rank 2 built from the spin and space degrees of freedom. Both terms are present in the nonrelativistic and relativized quark models, in which the  $SU_{sf}(6)$  spin-flavor symmetry is broken by the hyperfine interaction (Eq. (5.26) corresponds to the tensor component of the hyperfine interaction). Although in the present analysis we do not consider the contributions of the spin-orbit and the tensor interactions, we note that in the algebraic approach they can be taken into account without any difficulty.

## 6 Comparison with experimental mass spectrum

The mass formulas derived in Section 5 can be used to analyze the experimental mass spectrum of baryons. Here we discuss the mass spectrum of the nonstrange baryons belonging to the N and  $\Delta$  families in terms of the mass formula

$$M^2 = M_0^2 + (\kappa_1 N) n_u + (\kappa_2 N) (n_v + n_w) + \alpha L + a \left[ \langle \hat{C}_2(SU_{sf}(6)) \rangle - 45 \right] + b \left[ \langle \hat{C}_2(SU_f(3)) \rangle - 9 \right] + c \left[ \langle \hat{C}_2(SU_s(2)) \rangle - \frac{3}{4} \right]. \quad (6.1)$$

In this form we have absorbed all constant terms into  $M_0^2$ . We do not include interaction terms that mix the space and internal degrees of freedom. The seven coefficients are obtained by a fit to the data

$$\begin{aligned} M_0^2 &= 0.882, & \kappa_1 N &= 1.192, & \kappa_2 N &= 1.535, \\ \alpha &= 1.064, & a &= -0.042, & b &= 0.030, & c &= 0.124. \end{aligned} \quad (6.2)$$

All values are in  $\text{GeV}^2$ . The results are given in Table II. We have assigned the Roper resonance  $N(1440)P_{11}$ , the  $\Delta(1600)P_{33}$  and the  $\Delta(1900)S_{31}$  to the symmetric stretching vibration  $(n_u, n_v + n_w) = (1, 0)$  and the resonance  $N(1710)P_{11}$  to the  $(n_u, n_v + n_w) = (0, 1)$  vibration. The remaining part of the assignments is straightforward as rotational members of the ground band  $(n_u, n_v + n_w) = (0, 0)$ . In Table II we list all well-established (3 and 4 star) nucleon and delta resonances. We find a good overall fit for these resonances with an r.m.s. deviation of  $\delta_{\text{rms}} = 39$  MeV. Some of the results are also presented in Figure 5 in a standard Chew-Frautschi plot of baryon resonances [20].

It is worthwhile at this stage to comment on the results of Table II. We find that the spin-orbit interaction is not required by the data. In the quark model, where this term is introduced by the one-gluon exchange interaction, other mechanisms have to be found to cancel this contribution (called the ‘spin-orbit crisis’). We find instead that the ‘signature dependent’ terms are crucial in obtaining a good description of the data. In the quark model, this problem is solved either by using harmonic oscillator frequencies which are different for P-wave and D-wave baryons [4], or by giving only a qualitative description which is somewhat lower for P-wave and somewhat higher for D-wave baryons [5]. This situation is illustrated in Figure 6. The absence of the spin-orbit interaction is evident in the data (states with the same  $L, S$  and  $|L - S| \leq J \leq L + S$  have the same mass). For comparison, in Figure 6 we also show the results of [5]. Finally the value we find for  $\alpha$ , the slope of the Regge trajectory, is almost identical to that found in mesons [22]

$$\begin{aligned} \alpha_{\text{meson}} &= 1.081 \text{ GeV}^2, \\ \alpha_{\text{baryon}} &= 1.064 \text{ GeV}^2. \end{aligned} \quad (6.3)$$

This is consistent with QCD ideas which indicate a universal slope for both baryons and mesons [15]. The strength of the spin-spin interaction is also almost identical to that found in mesons:  $c_{\text{meson}} = 0.118 \text{ GeV}^2$  and  $c_{\text{baryon}} = 0.124 \text{ GeV}^2$ .

For completeness, we give in Tables III and IV all calculated nucleon and delta resonances below 2 GeV. The lowest missing states in the nucleon sector are the antisymmetric  $[20, 1^+]$  ones. As one can see from these tables, only a fraction of these resonances have been observed. This

problem of missing states is known to exist in quark potential models as well. The resonances in square brackets are not well established experimentally (1 and 2 star) and are tentatively assigned in the tables as candidates for some of the missing states. We shall return to the question of why some of the resonances have not been observed in a later publication, which includes a calculation of the strong decay widths.

To summarize, we have applied a collective string-like model to the nonstrange baryon resonances and found good overall agreement with the observed masses. The fit is of comparable quality to that obtained in quark potential models [4, 5], although the underlying dynamics is quite different. This shows that masses alone are not sufficient to distinguish between different forms of quark dynamics, *e.g.* single-particle *vs.* collective motion.

## 7 Electromagnetic couplings

Electromagnetic couplings are of crucial importance in unraveling the structure of hadrons, since they are far more sensitive to wave functions (and models) than masses. It has become customary to characterize the transverse couplings by the helicity amplitudes,  $A_{1/2}$  and  $A_{3/2}$ . These amplitudes are measurable in photo- and electroproduction. Their study is a major part of the experimental program at the new electron facilities [23].

Helicity amplitudes can be computed within the framework discussed here by (i) writing down the transition operator in terms of the constituent coordinates and momenta, (ii) rewriting them in terms of Jacobi coordinates and momenta, (iii) mapping the operators onto elements of the algebra and (iv) evaluating their matrix elements algebraically. A major problem in step (i) is what is precisely the form of the electromagnetic coupling. This form is usually obtained by a nonrelativistic reduction of the coupling of the point-like particles to the electromagnetic field. This gives a transition operator of the form [24, 25]

$$\mathcal{H} = \mathcal{H}_{\text{nr}} + \mathcal{H}_{\text{so}} + \mathcal{H}_{\text{na}} + \dots, \quad (7.1)$$

containing the contributions of the nonrelativistic part, the spin-orbit part and the nonadditive part associated with Wigner rotations [24] and higher order corrections,

$$\begin{aligned} \mathcal{H}_{\text{nr}} &= -\sum_{j=1}^3 \left[ \frac{e_j}{2m_j} (\vec{p}_j \cdot \vec{A}_j + \vec{A}_j \cdot \vec{p}_j) + 2\mu_j \vec{s}_j \cdot (\vec{\nabla} \times \vec{A}_j) \right], \\ \mathcal{H}_{\text{so}} &= -\sum_{j=1}^3 \mu_j \frac{1}{2m_j} \left( 2 - \frac{1}{g} \right) \vec{s}_j \cdot (\vec{E}_j \times \vec{p}_j - \vec{p}_j \times \vec{E}_j), \\ \mathcal{H}_{\text{na}} &= \frac{1}{2M_T} \sum_{j>i=1}^3 \left( \frac{\vec{s}_i}{m_i} - \frac{\vec{s}_j}{m_j} \right) \cdot (e_j \vec{E}_j \times \vec{p}_i - e_i \vec{E}_i \times \vec{p}_j). \end{aligned} \quad (7.2)$$

where  $m_j$ ,  $e_j$ ,  $\vec{s}_j$  and  $\mu_j = ge_j/2m_j$  denote the mass, charge, spin and magnetic moment of the  $j$ -th constituent, respectively,  $M_T = \sum_i m_i$  and  $\vec{A}_j \equiv \vec{A}(\vec{r}_j)$ ,  $\vec{E}_j \equiv \vec{E}(\vec{r}_j)$ . For purposes of illustrating the results in a transparent way, we consider in this article only the contribution from the nonrelativistic part of the electromagnetic coupling,

$$\mathcal{H} = \mathcal{H}_{\text{nr}}. \quad (7.3)$$

The spin-orbit and non-additive contributions can be included without any problem and will be presented in a subsequent publication.

The momentum dependent terms in Eq. (7.2) are unsuited for calculations of electromagnetic couplings of the photon to an extended object, in which the charge and magnetic moment are not concentrated at a single point but distributed along the string. Thus, often a transformation is

made to coordinate dependent terms by replacing  $\vec{p}/m_q$  by  $ik_0\vec{r}$  [26, 27], where  $k_0 = E_f - E_i$  is the photon energy. The two terms in  $\mathcal{H}_{\text{nr}}$  have then the meaning of electric and magnetic contributions and reduce to the electric dipole and magnetic dipole transition operators in the long-wavelength limit. The transverse coupling is obtained by inserting the radiation field for the absorption of a righthanded photon with momentum  $\vec{k} = k\hat{z}$  and integrating over the center-of-mass coordinate to give

$$\mathcal{H}^t = 6\sqrt{\frac{\pi}{k_0}}\mu e_3 \left[ ks_{3,+}\hat{U} - \frac{1}{g}\hat{T}_+ \right], \quad (7.4)$$

Here  $(k_0, \vec{k})$  is the photon four-momentum with  $\vec{k} = \vec{P}_f - \vec{P}_i$ , and  $\vec{P}_i$  ( $\vec{P}_f$ ) is the momentum of the initial (final) baryon resonance. In the derivation we have used that for three identical constituents the symmetry of the wave functions allows one to write  $\mathcal{H} = 3\mathcal{H}_3$ . The operators  $\hat{T}$  and  $\hat{U}$  act only on the spatial part of the baryon wave function and are given by

$$\begin{aligned} \hat{U} &= e^{-ik\sqrt{\frac{2}{3}}\lambda_z}, \\ \hat{T}_m &= im_q k_0 \sqrt{\frac{2}{3}} \lambda_m e^{-ik\sqrt{\frac{2}{3}}\lambda_z}, \end{aligned} \quad (7.5)$$

with  $m = -1, 0, 1$ .

In addition to transverse couplings, one can also consider longitudinal and scalar couplings. The longitudinal coupling is obtained by inserting the radiation field for the absorption of a longitudinally polarized virtual photon in Eq. (7.2),

$$\mathcal{H}^l = 6\sqrt{\frac{2\pi}{k_0}}\mu e_3 \frac{1}{g} \hat{T}_z. \quad (7.6)$$

The scalar amplitudes are given by the matrix elements of the zero-component of the electromagnetic current four-vector [28]

$$\mathcal{H}^s = -3\sqrt{\frac{2\pi}{k_0}} e_3 e^{ikr_{3,z}}, \quad (7.7)$$

which after transforming to Jacobi coordinates and integrating over the baryon center-of-mass coordinate reduces to

$$\mathcal{H}^s = -3\sqrt{\frac{2\pi}{k_0}} e_3 \hat{U}. \quad (7.8)$$

In order to calculate helicity amplitudes in  $U(7)$  one has to express the transition operators in terms of algebraic operators. In the limit of large  $N$  the operators  $\hat{D}$  and  $\hat{A}$  of Eq. (3.5) become the coordinates and momenta (*i.e.* their matrix elements are precisely those of the coordinates and momenta in the coordinate representation). We thus make in general the replacement (mapping) [29]

$$\begin{aligned} \sqrt{\frac{2}{3}}\lambda_m &\rightarrow \beta \hat{D}_{\lambda,m}/X_D, \\ \sqrt{\frac{2}{3}}p_{\lambda,m} &\rightarrow \frac{1}{\zeta} \hat{A}_{\lambda,m}/X_A, \end{aligned} \quad (7.9)$$

and a similar replacement for  $\rho_m, p_{\rho,m}$  (not needed here). In Eq. (7.9),  $\beta$  and  $1/\zeta$  represent the scale of coordinates and momenta and  $X_D$  and  $X_A$  are normalization factors. Since we have

written the transition operators in terms of coordinates only, we need only to replace  $\lambda_m$  by  $\hat{D}_{\lambda,m}$ . With this replacement the transition operators  $\hat{T}_m$  and  $\hat{U}$  become

$$\begin{aligned}\hat{U} &= e^{-ik\beta\hat{D}_{\lambda,z}/X_D}, \\ \hat{T}_m &= \frac{im_q k_0 \beta}{2X_D} \left( \hat{D}_{\lambda,m} e^{-ik\beta\hat{D}_{\lambda,z}/X_D} + e^{-ik\beta\hat{D}_{\lambda,z}/X_D} \hat{D}_{\lambda,m} \right).\end{aligned}\quad (7.10)$$

The normalization factor is given by the reduced matrix element of  $\hat{D}_\lambda$ ,

$$X_D = |\langle 1_\lambda^- | \hat{D}_\lambda | 0_S^+ \rangle|, \quad (7.11)$$

which away from the harmonic oscillator limit ( $R^2 > 0$ ) is given by

$$X_D \xrightarrow{N \rightarrow \infty} NR\sqrt{2}/(1+R^2). \quad (7.12)$$

In the harmonic oscillator limit discussed in Section 5 the normalization constant is  $X_D = \sqrt{3N}$  and the scale parameter  $\beta$  becomes the inverse of the oscillator size parameter  $\beta = 1/\alpha$  (see Appendix D).

The algebraic structure of the transverse, longitudinal and scalar couplings involves both the internal and the spatial degrees of freedom. In the long-wavelength limit the spatial part is linear in the generators of  $U(7)$ , but the more general form of Eq. (7.10) also contains an exponentiated generator. This poses a challenge to the calculation. Nonetheless, the calculation of the matrix elements of Eq. (7.10) is feasible, since they are related to the group elements of  $U(7)$ , *i.e.* a generalization of the familiar Wigner D-functions of  $SU(2)$ . This means that these matrix elements can be calculated exactly without having to make any further approximation. This holds for the harmonic oscillator which is a special case of  $U(7)$  as well, and thus allows one to do a straightforward calculation of helicity amplitudes in the quark model up to large number of quanta. Indeed, the fact that any observable can be calculated in a relatively straightforward way, is one of the main advantages of the algebraic method.

## 8 Calculation of helicity amplitudes

The calculation of the helicity amplitudes requires the evaluation of the matrix elements of the electromagnetic transition operator. We define the transverse helicity amplitudes  $A_\mu$ , with helicity  $\mu = 1/2$  and  $3/2$  in the usual fashion

$$\begin{aligned}A_{1/2} &= \langle \phi', L', S'; J', M'_J = 1/2 | \mathcal{H}^t | \phi, L, S; J = 1/2, M_J = -1/2 \rangle, \\ A_{3/2} &= \langle \phi', L', S'; J', M'_J = 3/2 | \mathcal{H}^t | \phi, L, S; J = 1/2, M_J = 1/2 \rangle.\end{aligned}\quad (8.1)$$

The longitudinal and scalar helicity amplitudes,  $A_l$  and  $A_s$ , are given by

$$\begin{aligned}A_l &= \langle \phi', L', S'; J', M'_J = 1/2 | \mathcal{H}^l | \phi, L, S; J = 1/2, M_J = 1/2 \rangle / \sqrt{2}, \\ A_s &= \langle \phi', L', S'; J', M'_J = 1/2 | \mathcal{H}^s | \phi, L, S; J = 1/2, M_J = 1/2 \rangle / \sqrt{2}.\end{aligned}\quad (8.2)$$

Here  $\phi$  indicates all additional quantum numbers needed to classify the states uniquely. The electromagnetic transition operator  $\mathcal{H}$  acts both on the spin-flavor part and the space part of the baryon wave functions. In the evaluation of the matrix elements we therefore separate these two parts by decoupling the wave functions

$$|\phi, L, S; J, M_J\rangle = \sum_{M_L, M_S} \langle L, M_L, S, M_S | J, M_J \rangle |\phi, L, M_L; S, M_S\rangle. \quad (8.3)$$

The spin-flavor part of the matrix elements is common to all models having the same spin-flavor structure and can be evaluated once and for all.

In general the helicity amplitudes can be expressed explicitly in terms of radial integrals. For the transverse couplings we have

$$A_\mu = \langle f | \mathcal{H}^t | i \rangle = \alpha_\mu \mathcal{A} + \beta_\mu \mathcal{B} , \quad (8.4)$$

where  $\mu$  denotes the helicity ( $\mu = 1/2, 3/2$ ). Here  $\mathcal{A}$  and  $\mathcal{B}$  represent the orbit- and spin-flip spatial amplitudes (radial integrals), respectively,

$$\begin{aligned} \mathcal{A} &= 6\sqrt{\frac{\pi}{k_0}} \mu \frac{1}{g} \langle f | \hat{T}_+ | i \rangle , \\ \mathcal{B} &= 6\sqrt{\frac{\pi}{k_0}} \mu k \langle f | \hat{U} | i \rangle . \end{aligned} \quad (8.5)$$

The nonrelativistic contribution to the longitudinal helicity amplitudes can be expressed in terms of a single spatial amplitude

$$A_l = \langle f | \mathcal{H}^l | i \rangle / \sqrt{2} = \gamma \mathcal{C} , \quad (8.6)$$

with

$$\mathcal{C} = 6\sqrt{\frac{\pi}{k_0}} \mu \frac{1}{g} \langle f | \hat{T}_z | i \rangle . \quad (8.7)$$

For the scalar helicity amplitudes we find

$$A_s = \langle f | \mathcal{H}^s | i \rangle / \sqrt{2} = \delta \mathcal{D} , \quad (8.8)$$

with

$$\mathcal{D} = -3\sqrt{\frac{\pi}{k_0}} \langle f | \hat{U} | i \rangle . \quad (8.9)$$

The coefficients  $\alpha_\mu$ ,  $\beta_\mu$ ,  $\gamma$  and  $\delta$  contain the contribution of the spin-flavor matrix element and of Clebsch-Gordan coefficients. By explicitly evaluating the matrix elements of the spin-flavor part with the conventions given in Appendix C, we obtain the coefficients for nucleon and delta resonances as shown in Tables V and VI. Some of these results have already been reported previously (see *e.g.* [24, 30]) and express the fact that all models of hadronic structure, that share the same spin-flavor structure, have the same form of the helicity amplitudes. The model dependence is contained in the actual expression for the spatial amplitudes,  $\mathcal{A}$ ,  $\mathcal{B}$ ,  $\mathcal{C}$  and  $\mathcal{D}$ . We therefore now turn to the calculation of these amplitudes in  $U(7)$ .

As one can see from the preceding discussion, all helicity amplitudes or form factors (transverse, longitudinal and scalar) can be expressed in terms of two types of elementary spatial matrix elements,

$$\begin{aligned} F(k) &= \langle f | \hat{U} | i \rangle , \\ G_m(k) &= \langle f | \hat{T}_m | i \rangle . \end{aligned} \quad (8.10)$$

These matrix elements contain all the hadron structure information. They are very sensitive to the hadron wave function. In photo- and electroproduction of baryon resonances only form factors in which the initial state is the nucleon (proton or neutron) can be measured. In Appendix D we show explicitly how  $F(k)$  and  $G_m(k)$  can be evaluated in  $U(7)$ .

## 9 Form factors in photo- and electroproduction

The important form factors in photo- and electroproduction are those connecting the ground state (the nucleon, proton or neutron) to its excited states. These form factors can be evaluated in explicit form in three different cases.

(i) Harmonic oscillator quark model.

In Table VII we present the elementary form factors,  $F(k)$  and  $G_m(k)$ , in the harmonic oscillator quark model. These form factors had been obtained previously [31, 24] in closed analytic form and are reported here for comparison with those of the collective model to be discussed next. The elastic form factor is given by

$$F(k) = e^{-k^2\beta^2/6} . \quad (9.1)$$

The scale parameter  $\beta$  is related to the harmonic oscillator size parameter  $\alpha$  by  $\beta = 1/\alpha$ .

(ii) Collective model: end string.

We consider first the case in which the charge and magnetic moment is concentrated at the end points of the string of Figure 1. For this case, the elastic form factor is given in terms of a spherical Bessel function (see Appendix D)

$$F(k) = j_0(k\beta) . \quad (9.2)$$

(iii) Collective model: distributed string.

We consider now the case in which the charge and magnetic moment are distributed along the strings of Figure 1 with a probability distribution

$$g(\beta) = \beta^2 e^{-\beta/a} . \quad (9.3)$$

In this case the form factors are obtained by integrating the form factors of case (ii). For the elastic form factor one has

$$F(k) = \int_0^\infty g(\beta) j_0(k\beta) d\beta / \int_0^\infty g(\beta) d\beta = \frac{1}{(1+k^2a^2)^2} . \quad (9.4)$$

In Tables VIII and IX we present analytic results for several transition form factors of the collective model for the end string and the distributed string, respectively (see Appendix D).

Comparing the elastic form factors for the three cases

$$F(k) = \begin{cases} e^{-k^2\beta^2/6} & \text{harmonic oscillator} & (R^2 = 0, N \rightarrow \infty) \\ j_0(k\beta) & \text{end string} & (R^2 > 0, N \rightarrow \infty) \\ 1/(1+k^2a^2)^2 & \text{distributed string} & (R^2 > 0, N \rightarrow \infty) \end{cases} \quad (9.5)$$

one can see that those of the string model drop as a power of  $k$ , while those of the harmonic oscillator drop exponentially with  $k$ . It is a major property of hadrons that form factors fall off as powers of  $k$ . This power behavior is naturally obtained in a collective string model, although the end string oscillates,  $j_0(k\beta) = \sin(k\beta)/k\beta$ . In order to obtain a similar behavior in quark models, a quark form factor is introduced and/or the wave function is boosted [32, 33].

We also note that all form factors are given in terms of one parameter describing the size of the hadron. This parameter can be determined from a measurement of the r.m.s. radius of the hadron. For  $k \rightarrow 0$  one has

$$F(k) \rightarrow \begin{cases} 1 - k^2\beta^2/6 + \dots \\ 1 - k^2\beta^2/6 + \dots \\ 1 - 2k^2a^2 + \dots \end{cases} \quad (9.6)$$

which gives the relation between the parameters,  $\beta$  and  $a$ , and the r.m.s. radius.



## 10 Comparison with experimental helicity amplitudes

The final step in comparing with experimental data is the choice of reference frame, which determines the relation between  $k^2$  and  $Q^2 = k^2 - k_0^2$ . We perform our calculations in the equal momentum or Breit frame (in which recoil contributions vanish),

$$k^2 = Q^2 + \frac{(W^2 - M^2)^2}{2(M^2 + W^2) + Q^2} . \quad (10.1)$$

$M$  is the nucleon mass,  $W$  is the mass of the resonance and  $-Q^2 = k_0^2 - k^2$  can be interpreted as the mass squared of the virtual photon.

In photoproduction one has  $Q^2 = 0$  and hence the photon momentum  $k = k_0$ . With this value of the momentum transfer  $k$  and the formalism of the preceding sections, we calculate the transverse helicity amplitudes for photoproduction. The results are presented in Tables X and XI. Calculation (1) is the harmonic oscillator result, whereas calculations (2) and (3) are the results of the distributed string with  $R^2 = 0.5$  and  $R^2 = 1.0$ , respectively. (We do not quote the results of the end string.) There are no free parameters in the calculation with the exception of a size parameter,  $\beta$  for (1) and  $a$  for (2) and (3). This size parameter is fixed by the value of the proton r.m.s. radius,  $\langle r^2 \rangle^{1/2} = 0.862 \pm 0.012$  fm [34]. The last column in Tables X and XI shows the experimental helicity amplitudes, quoted in [21] with a sign. This sign can neither be extracted from the data independently from the sign of the subsequent decay amplitude of the resonance ( $N^* \rightarrow N + \pi$ ) nor can be determined by calculations. It is thus a conventional sign (except for the relative sign of amplitudes leading to the same final state). In Tables X and XI we have used the signs of the harmonic oscillator limit (with the conventions of [43] for the harmonic oscillator wave functions), since the purpose of the present paper is to investigate different scenarios of hadronic structure in as much as possible model independent way. We note, however, that the sign conventions used by previous authors are often in disagreement with one another. In particular, the sign conventions of [35] are in disagreement with those of [17] and [24]. For example, in [24] the nonrelativistic contribution to the amplitude  $A_{1/2}^p$  leading to the state  $N(1720)P_{13}$  is calculated to be  $-113$ , while in [35] it is calculated to be  $+112$ . The comparison between theory and experiment in Tables X and XI should therefore be restricted to absolute values of the amplitudes (and their relative phases when leading to the same final states). With this in mind, the agreement with experimental data is fair and it is approximately the same for all calculations. The reason is that the photocouplings depend almost completely on the spin-flavor part. The dependence on the spatial part is minor, since the helicity amplitudes are evaluated at a relatively small momentum  $k = k_0$ , for which all calculations given similar results. To emphasize this point, consider the helicity amplitudes for the excitation of the  $\Delta(1232)P_{33}$  resonance. These can be written as

$$\begin{aligned} A_{1/2} &= -\frac{2}{3} \sqrt{\frac{2\pi}{k_0}} \mu k F(k) , \\ A_{3/2} &= -\frac{2}{3} \sqrt{\frac{6\pi}{k_0}} \mu k F(k) , \end{aligned} \quad (10.2)$$

where  $F(k)$  is given by Eq. (9.5). One first observes that the ratio  $A_{3/2}/A_{1/2} = \sqrt{3}$  is independent of  $k$ . This result is due to spin-flavor symmetry and is in good agreement with the experimental value  $1.83 \pm 0.15$ . Moreover, for small  $k$  the form factors are essentially identical, as one can see directly from Eq. (9.6).

We stress the fact that in the calculations we have insisted on describing correctly the proton r.m.s. radius. If this condition is relaxed, and  $\beta$  (or  $a$ ) is used as a parameter, a better description of the photocouplings can be obtained. The description can be improved further by changing the values of the  $g$ -factor (and accordingly the quark effective mass), as done in [35].

There are several places where there is a large disagreement between experiment and calculation. We mention here in particular the pair of states  $N(1535)S_{11}$  and  $N(1650)S_{11}$ . The disagreement

in this case can be corrected by mixing the two states [36, 33]

$$\begin{aligned} |N(1535)S_{11}\rangle &= +|^2 8_{1/2}\rangle \cos(-38^\circ) + |^4 8_{1/2}\rangle \sin(-38^\circ), \\ |N(1650)S_{11}\rangle &= -|^2 8_{1/2}\rangle \sin(-38^\circ) + |^4 8_{1/2}\rangle \cos(-38^\circ). \end{aligned} \quad (10.3)$$

This mixing breaks  $SU_{sf}(6)$  and can only be introduced by a tensor-like interaction, Eq. (5.26). It appears to be the only place in the spectrum and transitions where there is a clear evidence of such a breaking.

By comparing the photocouplings of the  $N(1440)P_{11}$  and the  $N(1710)P_{11}$  resonances for the harmonic oscillator and the collective string we see that in this case there is a clear difference between the two models. This is due to the different nature of these states: in the harmonic oscillator these states belong to the two-phonon multiplet whereas in the collective string they correspond to the fundamental (one-phonon) vibrations of the string.

Another observation is that the  $N(1520)D_{13}$  and  $N(1680)F_{15}$  resonances are predominantly excited with helicity  $\mu = 3/2$  for proton targets. The  $A_{1/2}^p$  amplitude is small because of a cancellation of the magnetic and electric contributions. Tables VII–IX show that this feature is present in both the collective string and the harmonic oscillator model. It appears to be a consequence of the spin-flavor symmetry and does not depend on details of the hadron structure.

Next we turn to a discussion of the transition form factors as are measured in electroproduction. It is here that major differences between the various models of hadron structure occur, since the form factors discussed in Section 9 differ widely for large  $k^2$  (or  $Q^2$ ). In Figure 7 we show a comparison between the experimental data for the proton elastic form factor and the form factors of Eq. (9.5). One can see clearly that only the form factor for the distributed string (dipole form factor) describes the data well. Similarly, we show in Figure 8 the transition form factor exciting the  $\Delta(1232)P_{33}$  resonance. Again it appears that the distributed string provides the best description. Figure 8 also indicates there is an additional contribution to  $G_M^\Delta$  of magnitude  $\sim 0.2 \times 3F_D$ , which falls off with  $Q^2$  faster than the leading order ( $Q^{-4}$ ).

Figures 9–12 show the helicity amplitudes for the  $N(1520)D_{13}$ ,  $N(1535)S_{11}$ ,  $N(1650)S_{11}$  and  $N(1680)F_{15}$  resonances. Although the experimental information is not very accurate, again it appears that the distributed string form factors describe the observed data better.

Since on one side the accurate measurement of transition form factors is part of the experimental programs at ELSA, MAMI and CEBAF and on the other side it is possible, with the methods discussed in this article, to compute any transition form factor, we believe that when the measurements will be completed, we will be able to make more definitive statements concerning the structure of the nucleon and its resonances and the validity of the various models of hadronic structure.

Finally, we note that, while the individual helicity amplitudes test models of hadronic structure, the helicity asymmetries

$$\frac{A_{1/2}^2 - A_{3/2}^2}{A_{1/2}^2 + A_{3/2}^2} \quad (10.4)$$

test more the form of the transition operator and the spin-flavor part of the wave functions. This is shown in Figures 13 and 14 where it is seen that both the harmonic oscillator quark model and the distributed string model give essentially the same results for the helicity asymmetries of the  $N(1520)D_{13}$  and the  $N(1680)F_{15}$  resonances.

## 11 Conclusions

We have presented here a framework within which different scenarios for baryon structure in the nonperturbative regime can be studied. This framework makes use of a spectrum generating

algebra

$$\mathcal{G} = U(7) \otimes SU_{sf}(6) \otimes SU_c(3) . \quad (11.1)$$

In particular, we have analyzed two different cases: (i) a ‘single-particle’ harmonic oscillator model and (ii) a ‘collective’ string model. We find that most results are independent of which model is used for the spatial part and are a consequence of the spin-flavor structure of the problem,  $SU_{sf}(6) \supset SU_f(3) \otimes SU_s(2)$ , and of the triality property of baryons, namely of the fact that there are three constituent parts which transform as the triplet representation of  $SU_c(3)$ . Differences between models occur only in the transition form factors which provide therefore an important clue to understand baryon structure. Present data suggest that the collective model with charge, mass and magnetic moment distributed along the string is the most likely description. New and more accurate data which can be obtained at new facilities like ELSA, MAMI and CEBAF may help elucidating the situation. The fact that the formalism has been set up in a as much as possible model independent way also gives the possibility to search for ‘new’ physics, which in this context means unconventional configurations of quarks and gluons.

The analysis presented in this article has been carried out assuming  $S_3$  (or  $D_3$ ) symmetry (*i.e.* three identical constituents with identical interactions). The next step in this study is the breaking of this symmetry. This is due to two effects: (i) the mass of the three constituents may not be the same; this breaking will allow us to treat strange baryons as well, and (ii) the interaction between the three objects may be such that the geometric arrangement is not that of an equilateral triangle with  $D_3$  symmetry; this breaking will allow us to discuss the electric form factor of the neutron, which is identically zero if the neutron has  $S_3$  symmetry. Both these types of symmetry breaking can be studied in the framework of the present formalism and will be discussed in more detail in the next publication in this series.

## Acknowledgements

This work is supported in part (RB) by the Stichting voor Fundamenteel Onderzoek der Materie (FOM) with financial support from the Nederlandse Organisatie voor Wetenschappelijk Onderzoek (NWO), (FI) by D.O.E. grant DE-FG02-91ER40608 and (AL) by the Israeli Science Ministry and by the Basic Research Foundation of the Israel Academy of Sciences and Humanities.

## A Basic matrix elements

The matrix elements of the mass-squared operator of Eq. (5.2) (and of all other  $U(7)$  operators of interest) can be calculated in either one of the two sets of basis states discussed in Section 4. With standard Racah algebra [39] they can be expressed in terms of the reduced matrix elements of the boson creation and annihilation operators themselves.

(i) In the harmonic oscillator  $U(4) \supset U(3)$  basis we have

$$\begin{aligned} \langle N, n', L' | b^\dagger | N-1, n, L \rangle &= \langle N-1, n, L | \tilde{b} | N, n', L' \rangle \\ &= \delta_{n', n+1} \begin{cases} \sqrt{(n+L+3)(L+1)} & \text{for } L' = L+1, \\ \sqrt{(n-L+2)L} & \text{for } L' = L-1, \end{cases} \\ \langle N, n', L' | s^\dagger | N-1, n, L \rangle &= \langle N-1, n, L | \tilde{s} | N, n', L' \rangle \\ &= \delta_{n', n} \delta_{L', L} \sqrt{N-n} . \end{aligned} \quad (\text{A.1})$$

(ii) In the  $U(4) \supset SO(4)$  basis we have [40]

$$\langle N, \omega', L' | c_l^\dagger | N-1, \omega, L \rangle = \langle N-1, \omega, L | \tilde{c}_l | N, \omega', L' \rangle$$

$$\begin{aligned}
&= \sqrt{(2L'+1)(2l+1)(2L+1)} \begin{Bmatrix} \omega'/2 & \omega'/2 & L' \\ \omega/2 & \omega/2 & L \\ 1/2 & 1/2 & l \end{Bmatrix} \\
&\quad \times \langle N, \omega' ||| c^\dagger ||| N-1, \omega \rangle, \tag{A.2}
\end{aligned}$$

where the  $SO(4)$  reduced (triple bar) matrix elements are

$$\langle N, \omega' ||| c^\dagger ||| N-1, \omega \rangle = \begin{cases} \sqrt{\omega(\omega+1)(N-\omega+1)/2} & \text{for } \omega' = \omega - 1, \\ \sqrt{(\omega+1)(\omega+2)(N+\omega+3)/2} & \text{for } \omega' = \omega + 1. \end{cases} \tag{A.3}$$

Here  $c_l^\dagger$  denotes for  $l = 0$  the scalar boson and for  $l = 1$  the vector boson.

## B Large N limit and coherent states

In the study of the properties of the string-like configuration of Figure 1, it is often convenient to introduce a coherent (or intrinsic) state basis. The use of this basis helps elucidating the physical content of algebraic models by stressing their geometry, and allows one to obtain closed analytic expressions for observables in the limit of large  $N$ . In view of confinement we expect  $N$  to be large, since  $N$  determines the number of bound states in the model.

Coherent states of  $U(k)$  are described in [10]. Here we need the coherent states of  $U(7)$  (the coset space  $U(7)/U(6) \otimes U(1)$ ). They are characterized by six complex variables. Removing overall rotations and considering static problems, one is left with only three real variables,  $(r_\rho, r_\lambda, \theta)$ : two radial coordinates and the angle inbetween. These variables characterize the shape of an object composed of three constituent parts and their geometric meaning is illustrated in Figure 15. The general properties of  $U(7)$  can be studied by using mean-field techniques. For a system of boson degrees of freedom, the variational wave function is a coherent state which take the form of a condensate of  $N$  bosons, which depends parametrically on the shape variables. The expectation value of an algebraic mass operator in this condensate defines a classical potential function  $V(r_\rho, r_\lambda, \theta)$ . The equilibrium shape parameters are defined by the global minimum of the potential function and are found by a variational calculation. Substituting these equilibrium values in the variational wave function provides an intrinsic state representing the equilibrium shape. For the  $S_3$ -invariant mass-squared operator of Eq. (5.2) the equilibrium shape parameters satisfy  $r_\rho = r_\lambda > 0$  and  $\theta = \pi/2$  [8]. These are precisely the conditions satisfied by the Jacobi coordinates of Eq. (2.2) for an equilateral triangular shape with a threefold symmetry axis (in our convention along the  $y$ -axis). In this case, the coherent state basis depends only on one variable,  $R = \sqrt{r_\rho^2 + r_\lambda^2}$ . It is obtained by introducing the following boson operators

$$\begin{aligned}
b_c^\dagger &= \frac{1}{\sqrt{1+R^2}} \left[ s^\dagger + R \frac{1}{\sqrt{2}} (b_{\rho,z}^\dagger + b_{\lambda,x}^\dagger) \right], \\
b_u^\dagger &= \frac{1}{\sqrt{1+R^2}} \left[ -R s^\dagger + \frac{1}{\sqrt{2}} (b_{\rho,z}^\dagger + b_{\lambda,x}^\dagger) \right], \\
b_v^\dagger &= \frac{1}{\sqrt{2}} (b_{\rho,z}^\dagger - b_{\lambda,x}^\dagger), \\
b_w^\dagger &= \frac{1}{\sqrt{2}} (b_{\rho,x}^\dagger + b_{\lambda,z}^\dagger), \\
b_1^\dagger &= \frac{1}{\sqrt{2}} (b_{\rho,y}^\dagger + b_{\lambda,y}^\dagger), \\
b_2^\dagger &= \frac{1}{\sqrt{2}} (-b_{\rho,x}^\dagger + b_{\lambda,z}^\dagger),
\end{aligned}$$

$$b_3^\dagger = \frac{1}{\sqrt{2}}(b_{\rho,y}^\dagger - b_{\lambda,y}^\dagger). \quad (\text{B.1})$$

The ground state of a system with  $S_3$  symmetry is represented by a condensate of the form

$$|N; R\rangle_c = \frac{1}{\sqrt{N!}}(b_c^\dagger)^N |0\rangle. \quad (\text{B.2})$$

This state contains several angular momentum states, since for  $R > 0$  the boson operator  $b_c^\dagger$  is a mixture of scalar and vector bosons. States with good quantum numbers are obtained by projection. For  $R = 0$  the boson condensate of Eq. (B.2) becomes the ground state of the harmonic oscillator

$$|N; R = 0\rangle = \frac{1}{\sqrt{N!}}(s^\dagger)^N |0\rangle, \quad (\text{B.3})$$

which contains only a single state with  $L^\pi = 0^+$ .

Excited states are obtained by replacing condensate bosons by other members of the basis Eq. (B.1). Vibrational excitations are represented by the  $b_u^\dagger$ ,  $b_v^\dagger$ ,  $b_w^\dagger$  boson operators [8], and are written as

$$\frac{1}{\mathcal{N}}(b_u^\dagger)^{n_u}(b_v^\dagger)^{n_v}(b_w^\dagger)^{n_w}(b_c^\dagger)^{N-n_u-n_v-n_w}|0\rangle, \quad (\text{B.4})$$

where  $\mathcal{N}$  is a normalization constant. The three rotational bosons  $b_1^\dagger$ ,  $b_2^\dagger$ ,  $b_3^\dagger$  represent instead spurious excitations of the condensate, corresponding to overall rotations (Goldstone modes).

## C Spin-flavor wave functions

In this appendix we list the conventions used for the spin and flavor wave functions.

(i) Spin wave functions [17]:

$$\begin{aligned} S = 1/2 \quad |\chi_{1/2}^\rho\rangle &= (|\uparrow\downarrow\uparrow\rangle - |\downarrow\uparrow\uparrow\rangle)/\sqrt{2}, \\ |\chi_{1/2}^\lambda\rangle &= (2|\uparrow\uparrow\downarrow\rangle - |\uparrow\downarrow\uparrow\rangle - |\downarrow\uparrow\uparrow\rangle)/\sqrt{6}, \\ S = 3/2 \quad |\chi_{3/2}^S\rangle &= |\uparrow\uparrow\uparrow\rangle. \end{aligned} \quad (\text{C.1})$$

We only show the state with the largest component of the projection  $M_S = S$ . The other states are obtained by applying the lowering operator in spin space.

(ii) Flavor wave functions [17]:

$$\begin{aligned} \text{octet} \quad |\phi_p^\rho\rangle &= (|udu\rangle - |duu\rangle)/\sqrt{2}, \\ |\phi_p^\lambda\rangle &= (2|uud\rangle - |udu\rangle - |duu\rangle)/\sqrt{6}, \\ \text{decuplet} \quad |\phi_{\Delta^{++}}^S\rangle &= |uuu\rangle. \end{aligned} \quad (\text{C.2})$$

We only show the highest charge state. The other charge states are obtained by applying the lowering operator in isospin space.

## D Radial integrals

All helicity amplitudes in  $U(7)$  are expressed in terms of two types of elementary spatial matrix elements (or radial integrals)

$$\begin{aligned} F(\epsilon) &= \langle f | \hat{U} | i \rangle = \langle f | e^{-i\epsilon \hat{D}_{\lambda,z}} | i \rangle, \\ G_m(\epsilon) &= \langle f | \hat{T}_m | i \rangle = \frac{i}{2} \eta \langle f | \hat{D}_{\lambda,m} e^{-i\epsilon \hat{D}_{\lambda,z}} + e^{-i\epsilon \hat{D}_{\lambda,z}} \hat{D}_{\lambda,m} | i \rangle. \end{aligned} \quad (\text{D.1})$$

Here  $\epsilon = k\beta/X_D$  and  $\eta = m_q k_0 \beta / X_D$  (see Eq. (7.10)). These matrix elements can be calculated exactly in  $U(7)$  by using the symmetry properties of the transition operator. We first discuss how they are calculated in general. Next we discuss two special cases for which they are derived in closed analytic form.

### D.1 General case

The most convenient basis to derive a general expression for the spatial matrix elements is the second one discussed in Section 4,

$$|N, (n_\rho, L_\rho), (\omega, L_\lambda); L, M_L\rangle. \quad (\text{D.2})$$

Since the operator  $\hat{D}_{\lambda,z}$  appearing in the exponent is a generator of  $SO_\lambda(4)$ , its matrix elements are diagonal in  $\omega$ . Moreover, since  $\hat{D}_{\lambda,m}$  does not depend on the  $\rho$ -coordinate, its matrix elements are also diagonal in the harmonic oscillator labels  $(n_\rho, L_\rho)$ . The matrix elements of  $\hat{U}$  can be evaluated by decoupling the  $\rho$ -part

$$\begin{aligned} F(\epsilon) &= \langle N, (n'_\rho, L'_\rho), (\omega', L'_\lambda); L', M'_L | e^{-i\epsilon \hat{D}_{\lambda,z}} | N, (n_\rho, L_\rho), (\omega, L_\lambda); L, M_L \rangle \\ &= \delta_{n'_\rho, n_\rho} \delta_{L'_\rho, L_\rho} \sum_{M_\rho, M_\lambda, M'_\lambda} \langle L_\rho, M_\rho, L'_\lambda, M'_\lambda | L', M'_L \rangle \langle L_\rho, M_\rho, L_\lambda, M_\lambda | L, M_L \rangle \\ &\quad \times \langle N - n_\rho, \omega', L'_\lambda, M'_\lambda | e^{-i\epsilon \hat{D}_{\lambda,z}} | N - n_\rho, \omega, L_\lambda, M_\lambda \rangle, \end{aligned} \quad (\text{D.3})$$

and by recognizing that the matrix elements appearing in the r.h.s. can be interpreted as representation matrix elements of  $SO(4)$ . (The projection of the angular momentum  $M_\rho, M_\lambda$  should not be confused with  $M_\rho, M_\lambda$  representation of  $S_3$ .) They can be derived by using the isomorphism between  $SO(4)$  and  $SU(2) \otimes SU(2)$  [41]

$$\begin{aligned} &\langle N, \omega', L', M'_L | e^{-i\epsilon \hat{D}_{\lambda,z}} | N, \omega, L, M_L \rangle = \\ &\quad \delta_{\omega', \omega} \delta_{M'_L, M_L} \sum_{\mu} \left\langle \frac{\omega}{2}, \mu, \frac{\omega}{2}, M_L - \mu \middle| L, M_L \right\rangle \left\langle \frac{\omega}{2}, \mu, \frac{\omega}{2}, M_L - \mu \middle| L', M'_L \right\rangle \\ &\quad \times \left[ \frac{1 + (-1)^{L+L'}}{2} \cos[(2\mu - M_L)\epsilon] - i \frac{1 - (-1)^{L+L'}}{2} \sin[(2\mu - M_L)\epsilon] \right]. \end{aligned} \quad (\text{D.4})$$

The matrix elements of  $\hat{T}_m$  are obtained in a similar way. Again we decouple the  $\rho$ -part of the wave function and then we insert a complete set of intermediate states to obtain

$$\begin{aligned} G_m(\epsilon) &= \langle N, (n'_\rho, L'_\rho), (\omega', L'_\lambda); L', M'_L | \hat{T}_m | N, (n_\rho, L_\rho), (\omega, L_\lambda); L, M_L \rangle \\ &= \frac{i}{2} \eta \delta_{n'_\rho, n_\rho} \delta_{L'_\rho, L_\rho} \sum_{M_\rho, M_\lambda, M'_\lambda} \langle L_\rho, M_\rho, L'_\lambda, M'_\lambda | L', M'_L \rangle \langle L_\rho, M_\rho, L_\lambda, M_\lambda | L, M_L \rangle \\ &\quad \times \sum_{L''_\lambda} \left[ \langle N - n_\rho, \omega', L'_\lambda, M'_\lambda | \hat{D}_{\lambda,m} | N - n_\rho, \omega, L''_\lambda, M_\lambda \rangle \right] \end{aligned}$$

$$\begin{aligned}
& \times \langle N - n_\rho, \omega, L''_\lambda, M_\lambda | e^{-i\epsilon \hat{D}_{\lambda,z}} | N - n_\rho, \omega, L_\lambda, M_\lambda \rangle \\
& + \langle N - n_\rho, \omega', L'_\lambda, M'_\lambda | e^{-i\epsilon \hat{D}_{\lambda,z}} | N - n_\rho, \omega', L''_\lambda, M'_\lambda \rangle \\
& \times \langle N - n_\rho, \omega', L''_\lambda, M'_\lambda | \hat{D}_{\lambda,m} | N - n_\rho, \omega, L_\lambda, M_\lambda \rangle \Big] . \quad (D.5)
\end{aligned}$$

The matrix elements of  $\hat{U}$  are given in Eq. (D.4), whereas those of  $\hat{D}_{\lambda,m}$  can be expressed in terms of their reduced matrix elements by using the Wigner-Eckart theorem

$$\langle N, \omega', L', M' | \hat{D}_m | N, \omega, L, M \rangle = \frac{\langle L, M, 1, m | L', M' \rangle}{\sqrt{2L'+1}} \langle N, \omega', L' || \hat{D} || N, \omega, L \rangle , \quad (D.6)$$

where

$$\begin{aligned}
\langle N, \omega', L' || \hat{D} || N, \omega, L \rangle &= \langle N, \omega, L || \hat{D} || N, \omega', L' \rangle \\
&= \delta_{\omega', \omega} \sqrt{(\omega - L)(\omega + L + 2)(L + 1)} \quad \text{for } L' = L + 1 . \quad (D.7)
\end{aligned}$$

The matrix element of  $\hat{T}_z$  can also be obtained in a more direct way by noting that

$$G_0(\epsilon) = -\eta \frac{dF(\epsilon)}{d\epsilon} . \quad (D.8)$$

## D.2 Harmonic oscillator

There exist special cases in which the matrix elements of the electromagnetic transition operator can be derived in closed analytic form. In this subsection we show how the well-known results of the harmonic oscillator quark model are obtained in  $U(7)$ . In this case, the most appropriate basis is the first one discussed in Section 4, namely

$$|N, (n_\rho, L_\rho), (n_\lambda, L_\lambda); L, M_L \rangle . \quad (D.9)$$

In the harmonic oscillator limit, the spatial part of the ground state wave function is

$$|[56, 0^+]_{0,0} \rangle \equiv |N, (0,0), (0,0), 0,0 \rangle . \quad (D.10)$$

The subscript indicates the harmonic oscillator shell quantum number  $n_\rho + n_\lambda$ . The spatial wave functions for some of the lowest excited states are

$$\begin{aligned}
|[70, 1^-]_{1, M_L} \rangle &\equiv |N, (0,0), (1,1), 1, M_L \rangle , \\
|[56, 0^+]_{2,0} \rangle &\equiv \frac{1}{\sqrt{2}} (|N, (2,0), (0,0), 0,0 \rangle + |N, (0,0), (2,0), 0,0 \rangle) , \\
|[70, 0^+]_{2,0} \rangle &\equiv \frac{1}{\sqrt{2}} (|N, (2,0), (0,0), 0,0 \rangle - |N, (0,0), (2,0), 0,0 \rangle) , \\
|[56, 2^+]_{2, M_L} \rangle &\equiv \frac{1}{\sqrt{2}} (|N, (2,2), (0,0), 2, M_L \rangle + |N, (0,0), (2,2), 2, M_L \rangle) , \\
|[70, 2^+]_{2, M_L} \rangle &\equiv \frac{1}{\sqrt{2}} (|N, (2,2), (0,0), 2, M_L \rangle - |N, (0,0), (2,2), 2, M_L \rangle) . \quad (D.11)
\end{aligned}$$

Just as in the general case, the matrix elements of  $\hat{U}$  and  $\hat{T}_m$  for the excitation of a baryon resonance from the ground state (nucleon) can be expressed in terms of  $U(4)$  matrix elements by decoupling the  $\rho$ -part

$$\begin{aligned}
\langle N, (n_\rho, L_\rho), (n_\lambda, L_\lambda); L, M_L | \left( \begin{array}{c} \hat{U} \\ \hat{T}_m \end{array} \right) | N, (0,0), (0,0), 0,0 \rangle = \\
\delta_{n_\rho,0} \delta_{L_\rho,0} \langle N, n_\lambda, L_\lambda, M_L | \left( \begin{array}{c} \hat{U} \\ \hat{T}_m \end{array} \right) | N, 0, 0, 0 \rangle . \quad (D.12)
\end{aligned}$$

The r.h.s. represents matrix elements in the harmonic oscillator  $U(4) \supset U(3)$  basis which are given by [42]

$$\begin{aligned}
\langle N, n, L, M_L | \hat{U} | N, 0, 0, 0 \rangle &= \delta_{M_L, 0} (-)^{(n-L)/2} \sqrt{\frac{N!(2L+1)}{(N-n)!(n+L+1)!(n-L)!}} \\
&\quad \times (\cos \epsilon)^{N-n} (-i \sin \epsilon)^n, \\
\langle N, n, L, M_L | \hat{T}_z | N, 0, 0, 0 \rangle &= i \eta \delta_{M_L, 0} (-)^{(n-L)/2} \sqrt{\frac{N!(2L+1)}{(N-n)!(n+L+1)!(n-L)!}} \\
&\quad \times (\cos \epsilon)^{N-n-1} (-i \sin \epsilon)^{n-1} (n - N \sin^2 \epsilon), \\
\langle N, n, L, M_L | \hat{T}_+ | N, 0, 0, 0 \rangle &= -i \eta \delta_{M_L, 1} (-)^{(n-L)/2} \sqrt{\frac{N!L(L+1)(2L+1)}{(N-n)!(n+L+1)!(n-L)!}} \\
&\quad \times (-i \sin \epsilon)^{n-1} \frac{1}{2} [(\cos \epsilon)^{N-n+1} + (\cos \epsilon)^{N-n}]. \quad (D.13)
\end{aligned}$$

We have used the sign conventions of [43] for the harmonic oscillator wave functions.

The elastic form factor is then given by

$$F(\epsilon) = \langle [56, 0^+]_{0,0} | \hat{U} | [56, 0^+]_{0,0} \rangle = (\cos \epsilon)^N \rightarrow e^{-k^2 \beta^2 / 6}. \quad (D.14)$$

In the last step we have taken the large  $N$  limit, which is such that  $n \ll N$  (where  $n$  denotes the oscillator shell), and  $\epsilon \sqrt{3N} (= k\beta)$  remains finite. For the harmonic oscillator we have  $\epsilon = k\beta / X_D = k\beta / \sqrt{3N}$ . For the inelastic transition to the first excited negative parity state we find

$$\begin{aligned}
G_+(\epsilon) = \langle [70, 1^-]_{1,1} | \hat{T}_+ | [56, 0^+]_{0,0} \rangle &= -i \eta \sqrt{N/2} [(\cos \epsilon)^N + (\cos \epsilon)^{N-1}] \\
&\rightarrow -i \sqrt{\frac{2}{3}} m_q k_0 \beta e^{-k^2 \beta^2 / 6}. \quad (D.15)
\end{aligned}$$

We have used  $\eta = m_q k_0 \beta / X_D = m_q k_0 \beta / \sqrt{3N}$ . From a comparison with the expressions derived in coordinate space we find that the scale parameter  $\beta$  is inversely proportional to the harmonic oscillator size parameter  $\alpha = 1/\beta$ .

In conclusion, we find that for  $N \rightarrow \infty$  the form factors in the harmonic oscillator limit of  $U(7)$  are identical to those in the harmonic oscillator quark model. The results are summarized in Table VII.

### D.3 Collective model

Also for the collective model discussed in Section 6 we can derive closed analytic expressions for some of the form factors. All rotational states belonging to the ground state band which has  $(n_u, n_v + n_w) = (0, 0)$  can be obtained from the ground state condensate of Eq. (B.2)

$$|N; R\rangle_c = \frac{1}{\sqrt{N!}} (b_c^\dagger)^N |0\rangle, \quad (D.16)$$

by projecting onto states of good angular momentum  $L$  and good permutation symmetry. Since the  $L^\pi = 0^+$  ground state is the only state with  $L = 0$ , one only has to project onto good angular momentum

$$|[56, 0^+]_{(0,0),0}\rangle \equiv \int d\Omega |N; R, \Omega\rangle_c Y_{00}(\Omega). \quad (D.17)$$

The subscript here denotes the vibrational quantum numbers  $(n_u, n_v + n_w)$  and  $Y_{LM_L}(\Omega)$  are the usual spherical harmonics.



The elastic form factor is then given by

$$\begin{aligned}
F(\epsilon) &= \langle [56, 0^+]_{(0,0)}, 0 | \hat{U} | [56, 0^+]_{(0,0)}, 0 \rangle \\
&= \int d\Omega d\Omega' Y_{00}^*(\Omega') {}_c \langle N; R, \Omega' | e^{-i\epsilon \hat{D}_{\lambda,z}} | N; R, \Omega \rangle_c Y_{00}(\Omega) .
\end{aligned} \tag{D.18}$$

Here the angle  $\Omega$  denotes the orientation of the condensate. For  $N \rightarrow \infty$  the matrix element in the integrand is diagonal in  $\Omega$  [44] and we find

$$\begin{aligned}
F(\epsilon) &\rightarrow \frac{1}{4\pi} \int d\Omega {}_c \langle N; R, \Omega | e^{-i\epsilon \hat{D}_{\lambda,z}} | N; R, \Omega \rangle_c \\
&\rightarrow \frac{1}{2} \int d(\cos \theta) e^{-i\epsilon [NR\sqrt{2}/(1+R^2)] \cos \theta} \\
&= j_0(k\beta) .
\end{aligned} \tag{D.19}$$

We have used that  $\epsilon = k\beta/X_D$  with  $X_D = NR\sqrt{2}/(1+R^2)$  for  $N \rightarrow \infty$ . In a similar way we find for the transition to the first excited negative parity state

$$\begin{aligned}
G_+(\epsilon) &= \langle [70, 1^-]_{(0,0)}, 1 | \hat{T}_+ | [56, 0^+]_{(0,0)}, 0 \rangle \\
&= \int d\Omega d\Omega' Y_{11}^*(\Omega') {}_c \langle N; R, \Omega' | \hat{T}_+ | N; R, \Omega \rangle_c Y_{00}(\Omega) \\
&\rightarrow -i\eta\sqrt{2} \frac{NR\sqrt{2}}{1+R^2} \frac{1}{4} \sqrt{3} \int d(\cos \theta) (1 - \cos^2 \theta) e^{-i\epsilon [NR\sqrt{2}/(1+R^2)] \cos \theta} \\
&= -i\sqrt{\frac{2}{3}} m_q k_0 \beta [j_0(k\beta) + j_2(k\beta)] .
\end{aligned} \tag{D.20}$$

For large  $N$  the intrinsic state for the first excited vibrational band with  $(n_u, n_v + n_w) = (1, 0)$ , the bandhead of which we have associated with the  $N(1440)P_{11}$  Roper and the  $\Delta(1600)P_{33}$  resonances, is given by

$$|N; R\rangle_u = b_u^\dagger \frac{1}{\sqrt{(N-1)!}} \left( b_c^\dagger \right)^{N-1} |0\rangle . \tag{D.21}$$

With the same methods as above we find that the spatial part of the transition form factor for the Roper resonance is given by

$$\begin{aligned}
F(\epsilon) &= \langle [56, 0^+]_{(1,0)}, 0 | \hat{U} | [56, 0^+]_{(0,0)}, 0 \rangle \\
&= \int d\Omega d\Omega' Y_{00}^*(\Omega') {}_u \langle N; R, \Omega' | e^{-i\epsilon \hat{D}_{\lambda,z}} | N; R, \Omega \rangle_c Y_{00}(\Omega) \\
&\rightarrow -i\epsilon \sqrt{\frac{N}{2}} \frac{1-R^2}{1+R^2} \frac{1}{2} \int d(\cos \theta) \cos \theta e^{-i\epsilon [NR\sqrt{2}/(1+R^2)] \cos \theta} \\
&= -\frac{1-R^2}{2R\sqrt{N}} k\beta j_1(k\beta) .
\end{aligned} \tag{D.22}$$

The results are summarized in Table VIII. For the more realistic case in which the charge and magnetic moment are not located at the ends of the string but rather distributed along the string, the matrix elements are obtained by folding the results of Table VIII with the probability distribution of Eq. (9.3). The corresponding results are presented in Table IX. For states with angular momentum  $L^\pi = 2^+$  one has to project, in addition to good angular momentum  $L$ , also to good permutation symmetry. We have not carried out the projection to good permutation symmetry explicitly. It only gives an overall multiplicative factor and does not change the  $k$  dependence of the matrix elements.

## References

- [1] M. GELL-MANN, *Phys. Rev.* **125**, 1067 (1962);  
Y. NE'EMAN, *Nucl. Phys.* **26**, 222 (1961).
- [2] A. ARIMA AND F. IACHELLO, *Phys. Rev. Lett.* **35**, 1069 (1975).
- [3] F. IACHELLO, *Chem. Phys. Lett.* **78**, 581 (1981).
- [4] N. ISGUR AND G. KARL, *Phys. Rev.* **D18**, 4187 (1978); **D19**, 2653 (1979); **D20**, 1191 (1979).
- [5] S. CAPSTICK AND N. ISGUR, *Phys. Rev.* **D34**, 2809 (1986).
- [6] For reviews see, in nuclear physics, F. IACHELLO AND A. ARIMA, "The Interacting Boson Model", Cambridge University Press, Cambridge (1987), and, in molecular physics, F. IACHELLO AND R.D. LEVINE, "Algebraic Theory of Molecules", Oxford University Press, Oxford (1993).
- [7] F. IACHELLO, *Nucl. Phys.* **A560**, 23 (1993).
- [8] R. BIJKER AND A. LEVIATAN, in "Symmetries in Science VII: Spectrum Generating Algebras and Dynamic Symmetries in Physics", ed. B. Gruber, Plenum Press, New York, in press; Proceedings of the XVI Oaxtepec Nuclear Physics Symposium, *Revista Mexicana de Fisica* **39**, Suplemento 2, 7 (1993).
- [9] R. BIJKER, A.E.L. DIEPERINK AND A. LEVIATAN, in "Symmetries in Science VII: Spectrum Generating Algebras and Dynamic Symmetries in Physics", ed. B. Gruber, Plenum Press, New York, in press.
- [10] See *e.g.* R. GILMORE AND D.H. FENG, *Nucl. Phys.* **A301**, 189 (1978);  
A.M. PERELOMOV, "Generalized coherent states and their applications", Springer Verlag (1986);  
W.M. ZHANG, D.H. FENG AND R. GILMORE, *Rev. Mod. Phys.* **62**, 867 (1990).
- [11] K.C. BOWLER, P.J. CORVI, A.J.G. HEY, P.D. JARVIS AND R.C. KING, *Phys. Rev.* **D24**, 197 (1981); A.J.G. HEY AND R.L. KELLY, *Phys. Rep.* **96**, 71 (1983).
- [12] N. ISGUR, G. KARL AND R. KONIUK, *Phys. Rev. Lett.* **41**, 1269 (1978).
- [13] M.W. KIRSON AND A. LEVIATAN, *Phys. Rev. Lett.* **55**, 2846 (1985).
- [14] G. HERZBERG, "Molecular Spectra and Molecular Structure II: Infrared and Raman Spectra of Polyatomic Molecules", Van Nostrand Rheinhold, Princeton (1945).
- [15] K. JOHNSON AND C.B. THORN, *Phys. Rev.* **D13**, 1934 (1974);  
I. BARS AND A.J. HANSON, *Phys. Rev.* **D13**, 1744 (1974);  
S. CATTO AND F. GÜRSEY, *Lett. Nuovo Cimento* **35**, 241 (1982).
- [16] R.P. FEYNMAN, M. KISLINGER AND F. RAVNDAL, *Phys. Rev.* **D3**, 2706 (1971).
- [17] R. KONIUK AND N. ISGUR, *Phys. Rev. Lett.* **44**, 845 (1980).
- [18] F. GÜRSEY AND L.A. RADICATI, *Phys. Rev. Lett.* **13**, 173 (1964).
- [19] F.J. SQUIRES, *Nuovo Cimento* **25**, 242 (1962);  
A. MARTIN, *Phys. Lett.* **1**, 72 (1962).
- [20] G.F. CHEW AND S.C. FRAUTSCHI, *Phys. Rev. Lett.* **7**, 394 (1961).

- [21] PARTICLE DATA GROUP, *Phys. Rev.* **D45**, S1 (1992).
- [22] F. IACHELLO, N.C. MUKHOPADHYAY AND L. ZHANG, *Phys. Lett.* **256B**, 295 (1991); *Phys. Rev.* **D44**, 898 (1991).
- [23] V.D. BURKERT, *Int. J. of Mod. Phys.* **E1**, 421 (1992).
- [24] F.E. CLOSE AND Z. LI, *Phys. Rev.* **D42**, 2194 (1990).
- [25] M. WARNS, H. SCHRÖDER, W. PFEIL AND H. ROLLNIK, *Z. Phys.* **C45**, 613 (1990).
- [26] R. MCCLARY AND N. BYERS, *Phys. Rev.* **D28**, 1692 (1983).
- [27] F. IACHELLO AND D. KUSNEZOV, *Phys. Rev.* **D45**, 4156 (1992).
- [28] M. BOURDEAU AND N. MUKHOPADHYAY, *Phys. Rev. Lett.* **58**, 976 (1987);  
S. CAPSTICK AND G. KARL, *Phys. Rev.* **D41**, 2767 (1990).
- [29] O.S. VAN ROOSMALEN AND A.E.L. DIEPERINK, *Ann. Phys. (N.Y.)* **139**, 198 (1982).
- [30] R. SARTOR AND F. STANCU, *Phys. Rev.* **D33**, 727 (1986).
- [31] L.A. COPLEY, G. KARL AND E. OBRYK, *Nucl. Phys.* **13**, 303 (1969).
- [32] A. LICHT AND A. PAGNAMENTA, *Phys. Rev.* **D2**, 1150 (1982).
- [33] F. FOSTER AND G. HUGHES, *Z. Phys.* **C14**, 123 (1982).
- [34] G.G. SIMON, C. SCHMITT, F. BORKOWSKI AND V.H. WALTER, *Nucl. Phys.* **A333**, 381 (1980).
- [35] S. CAPSTICK, *Phys. Rev.* **D46**, 2864 (1992).
- [36] A.J.G. HEY, P.J. LITCHFIELD AND R.J. CASHMORE, *Nucl. Phys.* **B95**, 516 (1975).
- [37] F. IACHELLO, A.D. JACKSON AND A. LANDE, *Phys. Lett.* **B43**, 191 (1973).
- [38] V.D. BURKERT, preprint CEBAF-PR-88-012.
- [39] See *e.g.* A. DESHALIT AND I. TALMI, “Nuclear Shell Theory”, Academic Press, New York (1963).
- [40] K.T. HECHT AND S.C. PANG, *J. Math. Phys.* **10**, 1571 (1979).
- [41] R. BIJKER AND R.D. AMADO, *Phys. Rev.* **A37**, 1425 (1988);  
L. BIEDENHARN, *J. Math. Phys.* **2**, 433 (1961).
- [42] R. BIJKER, R.D. AMADO AND D.A. SPARROW, *Phys. Rev.* **A33**, 871 (1986).
- [43] M. MOSHINSKY, “The Harmonic Oscillator in Modern Physics: From Atoms to Quarks”, Gordon and Breach (1969).
- [44] R. BIJKER AND R.D. AMADO, *Phys. Rev.* **A34**, 71 (1986).

Table I: Transformation properties under  $S_3$  of boson creation operators, generators of the algebra of  $U(7)$  and boson-pair creation operators. Here  $l = 0, 1, 2$  and  $l' = 0, 2$ .

Operator	$S_3$
$s^\dagger$ $\hat{n}_s, \hat{G}_S^{(l)}$ $(b_\rho^\dagger \times b_\rho^\dagger + b_\lambda^\dagger \times b_\lambda^\dagger)^{(l')}$	$S$
$b_\rho^\dagger$ $\hat{D}_\rho, \hat{A}_\rho, \hat{G}_{M_\rho}^{(l)}$ $(b_\rho^\dagger \times b_\lambda^\dagger + b_\lambda^\dagger \times b_\rho^\dagger)^{(l')}$	$M_\rho$
$b_\lambda^\dagger$ $\hat{D}_\lambda, \hat{A}_\lambda, \hat{G}_{M_\lambda}^{(l)}$ $(b_\rho^\dagger \times b_\rho^\dagger - b_\lambda^\dagger \times b_\lambda^\dagger)^{(l')}$	$M_\lambda$
$\hat{G}_A^{(l)}$ $(b_\rho^\dagger \times b_\lambda^\dagger - b_\lambda^\dagger \times b_\rho^\dagger)^{(1)}$	$A$

Table II: Mass spectrum of nonstrange baryon resonances of the nucleon and delta family in the collective string model. Here  $(n_1, n_2) = (n_u, n_v + n_w)$  denote the vibrational quantum numbers,  $K$  is the projection of the angular momentum  $L$ ,  $\pi$  is the parity,  $t$  is the transformation property under the point group  $D_3$ , and  $S$  denotes the spin. The masses are given in MeV. The experimental values are taken from [21].

Baryon	Status	Mass	$J^\pi$	$(n_1, n_2)$	$L^\pi, K$	$S$	$t$	$M_{\text{calc}}$
N(939) $P_{11}$	****	939	$\frac{1}{2}^+$	(0,0)	$0^+, 0$	$\frac{1}{2}$	$A_1$	939
N(1440) $P_{11}$	****	1430-1470	$\frac{1}{2}^+$	(1,0)	$0^+, 0$	$\frac{1}{2}$	$A_1$	1440
N(1520) $D_{13}$	****	1515-1530	$\frac{3}{2}^-$	(0,0)	$1^-, 1$	$\frac{1}{2}$	$E$	1566
N(1535) $S_{11}$	****	1520-1555	$\frac{1}{2}^-$	(0,0)	$1^-, 1$	$\frac{1}{2}$	$E$	1566
N(1650) $S_{11}$	****	1640-1680	$\frac{1}{2}^-$	(0,0)	$1^-, 1$	$\frac{3}{2}$	$E$	1680
N(1675) $D_{15}$	****	1670-1685	$\frac{5}{2}^-$	(0,0)	$1^-, 1$	$\frac{3}{2}$	$E$	1680
N(1680) $F_{15}$	****	1675-1690	$\frac{5}{2}^+$	(0,0)	$2^+, 0$	$\frac{1}{2}$	$A_1$	1735
N(1700) $D_{13}$	***	1650-1750	$\frac{3}{2}^-$	(0,0)	$1^-, 1$	$\frac{3}{2}$	$E$	1680
N(1710) $P_{11}$	***	1680-1740	$\frac{1}{2}^+$	(0,1)	$0^+, 0$	$\frac{1}{2}$	$E$	1710
N(1720) $P_{13}$	****	1650-1750	$\frac{3}{2}^+$	(0,0)	$2^+, 0$	$\frac{1}{2}$	$A_1$	1735
N(2190) $G_{17}$	****	2100-2200	$\frac{7}{2}^-$	(0,0)	$3^-, 1$	$\frac{1}{2}$	$E$	2140
N(2220) $H_{19}$	****	2180-2310	$\frac{9}{2}^+$	(0,0)	$4^+, 0$	$\frac{1}{2}$	$A_1$	2267
N(2250) $G_{19}$	****	2170-2310	$\frac{9}{2}^-$	(0,0)	$3^-, 1$	$\frac{3}{2}$	$E$	2225
N(2600) $I_{1,11}$	***	2550-2750	$\frac{11}{2}^-$	(0,0)	$5^-, 1$	$\frac{1}{2}$	$E$	2590
$\Delta(1232)P_{33}$	****	1230-1234	$\frac{3}{2}^+$	(0,0)	$0^+, 0$	$\frac{3}{2}$	$A_1$	1232
$\Delta(1600)P_{33}$	***	1550-1700	$\frac{3}{2}^+$	(1,0)	$0^+, 0$	$\frac{3}{2}$	$A_1$	1646
$\Delta(1620)S_{31}$	****	1615-1675	$\frac{1}{2}^-$	(0,0)	$1^-, 1$	$\frac{1}{2}$	$E$	1649
$\Delta(1700)D_{33}$	****	1670-1770	$\frac{3}{2}^-$	(0,0)	$1^-, 1$	$\frac{1}{2}$	$E$	1649
$\Delta(1900)S_{31}$	***	1850-1950	$\frac{1}{2}^-$	(1,0)	$1^-, 1$	$\frac{1}{2}$	$E$	1977
$\Delta(1905)F_{35}$	****	1870-1920	$\frac{5}{2}^+$	(0,0)	$2^+, 0$	$\frac{3}{2}$	$A_1$	1909
$\Delta(1910)P_{31}$	****	1870-1920	$\frac{1}{2}^+$	(0,0)	$2^+, 0$	$\frac{3}{2}$	$A_1$	1909
$\Delta(1920)P_{33}$	***	1900-1970	$\frac{3}{2}^+$	(0,0)	$2^+, 0$	$\frac{3}{2}$	$A_1$	1909
$\Delta(1930)D_{35}$	***	1920-1970	$\frac{5}{2}^-$	(0,0)	$2^-, 1$	$\frac{1}{2}$	$E$	1945
$\Delta(1950)F_{37}$	****	1940-1960	$\frac{7}{2}^+$	(0,0)	$2^+, 0$	$\frac{3}{2}$	$A_1$	1909
$\Delta(2420)H_{3,11}$	****	2300-2500	$\frac{11}{2}^+$	(0,0)	$4^+, 0$	$\frac{3}{2}$	$A_1$	2403

Table III: All calculated nucleon resonances (in MeV) below 2 GeV in the collective string model. Tentative assignments of 1 and 2 star resonances are shown in brackets.

State	$(n_1, n_2)$	$K$	$M_{\text{calc}}$	Baryon
${}^2_8_{1/2}[56, 0^+]$	(0,0)	0	939	N(939) $P_{11}$
${}^2_8_{1/2}[70, 1^-]$	(0,0)	1	1566	N(1535) $S_{11}$
${}^2_8_{3/2}[70, 1^-]$	(0,0)	1	1566	N(1520) $D_{13}$
${}^4_8_{1/2}[70, 1^-]$	(0,0)	1	1680	N(1650) $S_{11}$
${}^4_8_{3/2}[70, 1^-]$	(0,0)	1	1680	N(1700) $D_{13}$
${}^4_8_{5/2}[70, 1^-]$	(0,0)	1	1680	N(1675) $D_{15}$
${}^2_8_{1/2}[20, 1^+]$	(0,0)	0	1720	
${}^2_8_{3/2}[20, 1^+]$	(0,0)	0	1720	
${}^2_8_{3/2}[56, 2^+]$	(0,0)	0	1735	N(1720) $P_{13}$
${}^2_8_{5/2}[56, 2^+]$	(0,0)	0	1735	N(1680) $F_{15}$
${}^2_8_{3/2}[70, 2^-]$	(0,0)	1	1875	
${}^2_8_{5/2}[70, 2^-]$	(0,0)	1	1875	
${}^2_8_{3/2}[70, 2^+]$	(0,0)	2	1875	[N(1900) $P_{13}$ ]
${}^2_8_{5/2}[70, 2^+]$	(0,0)	2	1875	[N(2000) $F_{15}$ ]
${}^4_8_{1/2}[70, 2^-]$	(0,0)	1	1972	
${}^4_8_{3/2}[70, 2^-]$	(0,0)	1	1972	
${}^4_8_{5/2}[70, 2^-]$	(0,0)	1	1972	
${}^4_8_{7/2}[70, 2^-]$	(0,0)	1	1972	
${}^4_8_{1/2}[70, 2^+]$	(0,0)	2	1972	
${}^4_8_{3/2}[70, 2^+]$	(0,0)	2	1972	
${}^4_8_{5/2}[70, 2^+]$	(0,0)	2	1972	
${}^4_8_{7/2}[70, 2^+]$	(0,0)	2	1972	[N(1990) $F_{17}$ ]
${}^2_8_{1/2}[56, 0^+]$	(1,0)	0	1440	N(1440) $P_{11}$
${}^2_8_{1/2}[70, 1^-]$	(1,0)	1	1909	
${}^2_8_{3/2}[70, 1^-]$	(1,0)	1	1909	
${}^2_8_{1/2}[70, 0^+]$	(0,1)	0	1710	N(1710) $P_{11}$
${}^4_8_{3/2}[70, 0^+]$	(0,1)	0	1815	
${}^2_8_{1/2}[56, 1^-]$	(0,1)	1	1866	
${}^2_8_{3/2}[56, 1^-]$	(0,1)	1	1866	
${}^2_8_{1/2}[70, 1^+]$	(0,1)	0	1997	
${}^2_8_{3/2}[70, 1^+]$	(0,1)	0	1997	
${}^2_8_{1/2}[70, 1^-]$	(0,1)	1	1997	
${}^2_8_{3/2}[70, 1^-]$	(0,1)	1	1997	

Table IV: All calculated delta resonances (in MeV) below 2 GeV in the collective string model. Tentative assignments of 1 and 2 star resonances are shown in brackets.

State	$(n_1, n_2)$	$K$	$M_{\text{calc}}$	Baryon
${}^4 10_{3/2}[56, 0^+]$	(0,0)	0	1232	$\Delta(1232)P_{33}$
${}^2 10_{1/2}[70, 1^-]$	(0,0)	1	1649	$\Delta(1620)S_{31}$
${}^2 10_{3/2}[70, 1^-]$	(0,0)	1	1649	$\Delta(1700)D_{33}$
${}^4 10_{1/2}[56, 2^+]$	(0,0)	0	1909	$\Delta(1910)P_{31}$
${}^4 10_{3/2}[56, 2^+]$	(0,0)	0	1909	$\Delta(1920)P_{33}$
${}^4 10_{5/2}[56, 2^+]$	(0,0)	0	1909	$\Delta(1905)F_{35}$
${}^4 10_{7/2}[56, 2^+]$	(0,0)	0	1909	$\Delta(1950)F_{37}$
${}^2 10_{3/2}[70, 2^-]$	(0,0)	1	1945	$[\Delta(1940)D_{33}]$
${}^2 10_{5/2}[70, 2^-]$	(0,0)	1	1945	$\Delta(1930)D_{35}$
${}^2 10_{3/2}[70, 2^+]$	(0,0)	2	1945	
${}^2 10_{5/2}[70, 2^+]$	(0,0)	2	1945	$[\Delta(2000)F_{35}]$
${}^4 10_{3/2}[56, 0^+]$	(1,0)	0	1646	$\Delta(1600)P_{33}$
${}^2 10_{1/2}[70, 1^-]$	(1,0)	1	1977	$\Delta(1900)S_{31}$
${}^2 10_{3/2}[70, 1^-]$	(1,0)	1	1977	
${}^2 10_{1/2}[70, 0^+]$	(0,1)	0	1786	$[\Delta(1750)P_{31}]$

Table V: Spin-flavor coefficients of  $\mathcal{H}_{\text{NR}}$  in transverse, Eq. (8.4), longitudinal, Eq. (8.6), and scalar, Eq. (8.8), helicity amplitudes for nucleon resonances: proton- and neutron-target couplings.

State	$A_{1/2}^p$		$A_{3/2}^p$		$A_{1/2}^n$		$A_{3/2}^n$		$A_l^p (A_s^p)$	$A_l^n (A_s^n)$
	$\alpha_{1/2}$	$\beta_{1/2}$	$\alpha_{3/2}$	$\beta_{3/2}$	$\alpha_{1/2}$	$\beta_{1/2}$	$\alpha_{3/2}$	$\beta_{3/2}$	$\gamma(\delta)$	$\gamma(\delta)$
${}^2\mathbf{8}_{1/2}[56, 0^+]$	0	$\frac{1}{3}$	0	0	0	$-\frac{2}{9}$	0	0	$\frac{1}{3}$	0
${}^2\mathbf{8}_{3/2}[56, 2^+]$	$\frac{-1}{\sqrt{15}}$	$\frac{-\sqrt{2}}{3\sqrt{5}}$	$\frac{1}{3\sqrt{5}}$	0	0	$\frac{2\sqrt{2}}{9\sqrt{5}}$	0	0	$\frac{-\sqrt{2}}{3\sqrt{5}}$	0
${}^2\mathbf{8}_{5/2}[56, 2^+]$	$\frac{-\sqrt{2}}{3\sqrt{5}}$	$\frac{1}{\sqrt{15}}$	$\frac{-2}{3\sqrt{5}}$	0	0	$\frac{-2}{3\sqrt{15}}$	0	0	$\frac{1}{\sqrt{15}}$	0
${}^2\mathbf{8}_{1/2}[70, 0^+]$	0	$\frac{1}{3\sqrt{2}}$	0	0	0	$\frac{-1}{9\sqrt{2}}$	0	0	$\frac{1}{3\sqrt{2}}$	$\frac{-1}{3\sqrt{2}}$
${}^2\mathbf{8}_{1/2}[70, 1^-]$	$\frac{-1}{3\sqrt{3}}$	$\frac{-1}{3\sqrt{6}}$	0	0	$\frac{1}{3\sqrt{3}}$	$\frac{1}{9\sqrt{6}}$	0	0	$\frac{-1}{3\sqrt{6}}$	$\frac{1}{3\sqrt{6}}$
${}^2\mathbf{8}_{3/2}[70, 1^-]$	$\frac{-1}{3\sqrt{6}}$	$\frac{1}{3\sqrt{3}}$	$\frac{-1}{3\sqrt{2}}$	0	$\frac{1}{3\sqrt{6}}$	$\frac{-1}{9\sqrt{3}}$	$\frac{1}{3\sqrt{2}}$	0	$\frac{1}{3\sqrt{3}}$	$\frac{-1}{3\sqrt{3}}$
${}^2\mathbf{8}_{3/2}[70, 2^+]$	$\frac{-1}{\sqrt{30}}$	$\frac{-1}{3\sqrt{5}}$	$\frac{1}{3\sqrt{10}}$	0	$\frac{1}{\sqrt{30}}$	$\frac{1}{9\sqrt{5}}$	$\frac{-1}{3\sqrt{10}}$	0	$\frac{-1}{3\sqrt{5}}$	$\frac{1}{3\sqrt{5}}$
${}^2\mathbf{8}_{5/2}[70, 2^+]$	$\frac{-1}{3\sqrt{5}}$	$\frac{1}{\sqrt{30}}$	$\frac{-\sqrt{2}}{3\sqrt{5}}$	0	$\frac{1}{3\sqrt{5}}$	$\frac{-1}{3\sqrt{30}}$	$\frac{\sqrt{2}}{3\sqrt{5}}$	0	$\frac{1}{\sqrt{30}}$	$\frac{-1}{\sqrt{30}}$
${}^4\mathbf{8}_{3/2}[70, 0^+]$	0	0	0	0	0	$\frac{1}{9\sqrt{2}}$	0	$\frac{1}{3\sqrt{6}}$	0	0
${}^4\mathbf{8}_{1/2}[70, 1^-]$	0	0	0	0	0	$\frac{-1}{9\sqrt{6}}$	0	0	0	0
${}^4\mathbf{8}_{3/2}[70, 1^-]$	0	0	0	0	0	$\frac{-1}{9\sqrt{30}}$	0	$\frac{-1}{3\sqrt{10}}$	0	0
${}^4\mathbf{8}_{5/2}[70, 1^-]$	0	0	0	0	0	$\frac{1}{3\sqrt{30}}$	0	$\frac{1}{3\sqrt{15}}$	0	0
${}^4\mathbf{8}_{1/2}[70, 2^+]$	0	0	0	0	0	$\frac{1}{9\sqrt{10}}$	0	0	0	0
${}^4\mathbf{8}_{3/2}[70, 2^+]$	0	0	0	0	0	$\frac{-1}{9\sqrt{10}}$	0	$\frac{1}{3\sqrt{30}}$	0	0
${}^4\mathbf{8}_{5/2}[70, 2^+]$	0	0	0	0	0	$\frac{-1}{3\sqrt{210}}$	0	$\frac{-1}{\sqrt{105}}$	0	0
${}^4\mathbf{8}_{7/2}[70, 2^+]$	0	0	0	0	0	$\frac{1}{3\sqrt{35}}$	0	$\frac{1}{3\sqrt{21}}$	0	0
${}^2\mathbf{8}_{1/2}[20, 1^+]$	0	0	0	0	0	0	0	0	0	0
${}^2\mathbf{8}_{3/2}[20, 1^+]$	0	0	0	0	0	0	0	0	0	0



Table VI: Spin-flavor coefficients of  $\mathcal{H}_{\text{nr}}$  in transverse, Eq. (8.4), longitudinal, Eq. (8.6), and scalar, Eq. (8.8), helicity amplitudes for delta resonances.

State	$A_{1/2}^{p,n}$		$A_{3/2}^{p,n}$		$A_l^{p,n} (A_s^{p,n})$
	$\alpha_{1/2}$	$\beta_{1/2}$	$\alpha_{3/2}$	$\beta_{3/2}$	$\gamma (\delta)$
$^4 10_{3/2}[56, 0^+]$	0	$\frac{-\sqrt{2}}{9}$	0	$\frac{-\sqrt{2}}{3\sqrt{3}}$	0
$^4 10_{1/2}[56, 2^+]$	0	$\frac{-\sqrt{2}}{9\sqrt{5}}$	0	0	0
$^4 10_{3/2}[56, 2^+]$	0	$\frac{\sqrt{2}}{9\sqrt{5}}$	0	$\frac{-\sqrt{2}}{3\sqrt{15}}$	0
$^4 10_{5/2}[56, 2^+]$	0	$\frac{\sqrt{2}}{3\sqrt{105}}$	0	$\frac{2}{\sqrt{105}}$	0
$^4 10_{7/2}[56, 2^+]$	0	$\frac{-2}{3\sqrt{35}}$	0	$\frac{-2}{3\sqrt{21}}$	0
$^2 10_{1/2}[70, 0^+]$	0	$\frac{1}{9\sqrt{2}}$	0	0	$\frac{-1}{3\sqrt{2}}$
$^2 10_{1/2}[70, 1^-]$	$\frac{1}{3\sqrt{3}}$	$\frac{-1}{9\sqrt{6}}$	0	0	$\frac{1}{3\sqrt{6}}$
$^2 10_{3/2}[70, 1^-]$	$\frac{1}{3\sqrt{6}}$	$\frac{1}{9\sqrt{3}}$	$\frac{1}{3\sqrt{2}}$	0	$\frac{-1}{3\sqrt{3}}$
$^2 10_{3/2}[70, 2^+]$	$\frac{1}{\sqrt{30}}$	$\frac{-1}{9\sqrt{5}}$	$\frac{-1}{3\sqrt{10}}$	0	$\frac{1}{3\sqrt{5}}$
$^2 10_{5/2}[70, 2^+]$	$\frac{1}{3\sqrt{5}}$	$\frac{1}{3\sqrt{30}}$	$\frac{\sqrt{2}}{3\sqrt{5}}$	0	$\frac{-1}{\sqrt{30}}$

Table VII: Analytic expressions of the matrix elements of the transition operators of Eq. (7.10) in the harmonic oscillator limit of  $U(7)$  for  $N \rightarrow \infty$ . The initial state is  $[56, 0^+]_0$ .

Final state	$\langle f \hat{U} i\rangle$	$\langle f \hat{T}_z i\rangle/m_q k_0 \beta$	$\langle f \hat{T}_\pm i\rangle/m_q k_0 \beta$
$[56, 0^+]_0$	$e^{-k^2 \beta^2 / 6}$	$\frac{1}{3} k \beta e^{-k^2 \beta^2 / 6}$	0
$[70, 1^-]_1$	$-i \frac{1}{\sqrt{3}} k \beta e^{-k^2 \beta^2 / 6}$	$i \frac{1}{\sqrt{3}} (1 - \frac{k^2 \beta^2}{3}) e^{-k^2 \beta^2 / 6}$	$\mp i \sqrt{\frac{2}{3}} e^{-k^2 \beta^2 / 6}$
$[56, 0^+]_2$	$\frac{1}{6\sqrt{3}} k^2 \beta^2 e^{-k^2 \beta^2 / 6}$	$-\frac{1}{3\sqrt{3}} k \beta (1 - \frac{k^2 \beta^2}{6}) e^{-k^2 \beta^2 / 6}$	0
$[70, 0^+]_2$	$-\frac{1}{6\sqrt{3}} k^2 \beta^2 e^{-k^2 \beta^2 / 6}$	$\frac{1}{3\sqrt{3}} k \beta (1 - \frac{k^2 \beta^2}{6}) e^{-k^2 \beta^2 / 6}$	0
$[56, 2^+]_2$	$-\frac{1}{3\sqrt{6}} k^2 \beta^2 e^{-k^2 \beta^2 / 6}$	$\frac{2}{3\sqrt{6}} k \beta (1 - \frac{k^2 \beta^2}{6}) e^{-k^2 \beta^2 / 6}$	$\mp \frac{1}{3} k \beta e^{-k^2 \beta^2 / 6}$
$[70, 2^+]_2$	$\frac{1}{3\sqrt{6}} k^2 \beta^2 e^{-k^2 \beta^2 / 6}$	$-\frac{2}{3\sqrt{6}} k \beta (1 - \frac{k^2 \beta^2}{6}) e^{-k^2 \beta^2 / 6}$	$\pm \frac{1}{3} k \beta e^{-k^2 \beta^2 / 6}$

Table VIII: Analytic expressions of the matrix elements of the transition operators of Eq. (7.10) in the end string model for  $N \rightarrow \infty$ . The initial state is  $[56, 0^+]_{(0,0)}$ .

Final state	$\langle f \hat{U} i\rangle$	$\langle f \hat{T}_z i\rangle/m_q k_0 \beta$	$\langle f \hat{T}_\pm i\rangle/m_q k_0 \beta$
$[56, 0^+]_{(0,0)}$	$j_0(k\beta)$	$j_1(k\beta)$	0
$[70, 1^-]_{(0,0)}$	$-i\sqrt{3}j_1(k\beta)$	$i\frac{1}{\sqrt{3}}[j_0(k\beta) - 2j_2(k\beta)]$	$\mp i\sqrt{\frac{2}{3}}[j_0(k\beta) + j_2(k\beta)]$
$[56, 0^+]_{(1,0)}$	$-\frac{1-R^2}{2R\sqrt{N}}k\beta j_1(k\beta)$	$\frac{1-R^2}{6R\sqrt{N}}k\beta[2j_0(k\beta) - j_2(k\beta)]$	0
$[70, 0^+]_{(0,1)}$	$-\frac{1}{2}\sqrt{\frac{1+R^2}{NR^2}}k\beta j_1(k\beta)$	$\frac{1}{6}\sqrt{\frac{1+R^2}{NR^2}}k\beta[2j_0(k\beta) - j_2(k\beta)]$	0
$[56, 2^+]_{(0,0)}^a$	$-\sqrt{5}j_2(k\beta)$	$\frac{1}{\sqrt{5}}[2j_1(k\beta) - 3j_3(k\beta)]$	$\mp\sqrt{\frac{6}{5}}[j_1(k\beta) + j_3(k\beta)]$
$[70, 2^+]_{(0,0)}^a$	$-\sqrt{5}j_2(k\beta)$	$\frac{1}{\sqrt{5}}[2j_1(k\beta) - 3j_3(k\beta)]$	$\mp\sqrt{\frac{6}{5}}[j_1(k\beta) + j_3(k\beta)]$

<sup>a</sup> Up to an overall constant.

Table IX: Analytic expressions of the matrix elements of the transition operators of Eq. (7.10) in the distributed string model for  $N \rightarrow \infty$ .  $H(x) = \arctan x - x/(1+x^2)$ . The initial state is  $[56, 0^+]_{(0,0)}$ .

Final state	$\langle f \hat{U} i\rangle$	$\langle f \hat{T}_z i\rangle/m_q k_0 a$	$\langle f \hat{T}_\pm i\rangle/m_q k_0 a$
$[56, 0^+]_{(0,0)}$	$\frac{1}{(1+k^2 a^2)^2}$	$\frac{4ka}{(1+k^2 a^2)^3}$	0
$[70, 1^-]_{(0,0)}$	$-i\sqrt{3}\frac{ka}{(1+k^2 a^2)^2}$	$i\sqrt{3}\frac{1-3k^2 a^2}{(1+k^2 a^2)^3}$	$\mp i\sqrt{6}\frac{1}{(1+k^2 a^2)^2}$
$[56, 0^+]_{(1,0)}$	$-\frac{1-R^2}{R\sqrt{N}}\frac{2k^2 a^2}{(1+k^2 a^2)^3}$	$\frac{1-R^2}{R\sqrt{N}}\frac{4ka(1-2k^2 a^2)}{(1+k^2 a^2)^4}$	0
$[70, 0^+]_{(0,1)}$	$-\sqrt{\frac{1+R^2}{NR^2}}\frac{2k^2 a^2}{(1+k^2 a^2)^3}$	$\sqrt{\frac{1+R^2}{NR^2}}\frac{4ka(1-2k^2 a^2)}{(1+k^2 a^2)^4}$	0
$[56, 2^+]_{(0,0)}^a$	$-\sqrt{5}\left[\frac{-1}{(1+k^2 a^2)^2} + \frac{3}{2k^3 a^3}H(ka)\right]$	$\sqrt{5}\left[\frac{3+7k^2 a^2}{ka(1+k^2 a^2)^3} - \frac{9}{2k^4 a^4}H(ka)\right]$	$\mp\sqrt{30}\left[\frac{-1}{ka(1+k^2 a^2)^2} + \frac{3}{2k^4 a^4}H(ka)\right]$
$[70, 2^+]_{(0,0)}^a$	$-\sqrt{5}\left[\frac{-1}{(1+k^2 a^2)^2} + \frac{3}{2k^3 a^3}H(ka)\right]$	$\sqrt{5}\left[\frac{3+7k^2 a^2}{ka(1+k^2 a^2)^3} - \frac{9}{2k^4 a^4}H(ka)\right]$	$\mp\sqrt{30}\left[\frac{-1}{ka(1+k^2 a^2)^2} + \frac{3}{2k^4 a^4}H(ka)\right]$

<sup>a</sup> Up to an overall constant.

Table X: Helicity amplitudes  $A_\mu^{p,n}$  in  $10^{-3} \text{ GeV}^{-1/2}$  for nucleon resonances calculated in the Breit frame for  $R^2 = 0.0$  (harmonic oscillator) (1),  $R^2 = 0.5$  and  $R^2 = 1.0$  (distributed string), (2) and (3), respectively. The calculations are done in a model space with  $n_\rho + n_\lambda \leq N = 20$ . The quark mass  $m_q$  is  $M_p/2.793$ , which corresponds to  $g = 1$  and  $\mu = \mu_p = 0.13 \text{ GeV}^{-1}$ . The size parameters are obtained from the r.m.s. radius and are given by  $\beta = 0.855 \text{ fm}$ ,  $a = 0.242 \text{ fm}$  and  $a = 0.248 \text{ fm}$ , respectively. We have suppressed a factor of  $+i$  for the transitions to the negative parity states. The data are taken from [21].

Resonance	State	$\mu$	$A_\mu^{p,n}(\text{th})$			$A_\mu^{p,n}(\text{exp})$
			(1)	(2)	(3)	
N(1440) $P_{11}$	${}^2 8_{1/2}[56, 0^+]$	$p, 1/2$	+67	+12	+0	$-68 \pm 5$
		$n, 1/2$	-45	-8	-0	$+39 \pm 15$
N(1520) $D_{13}$	${}^2 8_{3/2}[70, 1^-]$	$p, 1/2$	-43	-42	-43	$-23 \pm 9$
		$n, 1/2$	-27	-27	-27	$-64 \pm 8$
		$p, 3/2$	+108	+107	+109	$+163 \pm 8$
		$n, 3/2$	-108	-107	-109	$-141 \pm 11$
N(1535) $S_{11}$	${}^2 8_{1/2}[70, 1^-]$	$p, 1/2$	+158	+160	+162	$+74 \pm 11$
			+125	+126	+127 <sup>a</sup>	
		$n, 1/2$	-109	-111	-112	$-72 \pm 25$
N(1650) $S_{11}$	${}^4 8_{1/2}[70, 1^-]$	$p, 1/2$	0	0	0	$+48 \pm 16$
			+75	+91	+91 <sup>a</sup>	
		$n, 1/2$	+21	+25	+25	$-17 \pm 37$
N(1675) $D_{15}$	${}^4 8_{5/2}[70, 1^-]$	$p, 1/2$	0	0	0	$+19 \pm 12$
		$n, 1/2$	-26	-33	-33	$-47 \pm 23$
		$p, 3/2$	0	0	0	$+19 \pm 12$
		$n, 3/2$	-37	-47	-47	$-69 \pm 19$
N(1680) $F_{15}$	${}^2 8_{5/2}[56, 2^+]$	$p, 1/2$	-6	-4	-4	$-17 \pm 10$
		$n, 1/2$	+55	+40	+40	$+31 \pm 13$
		$p, 3/2$	+109	+81	+80	$+127 \pm 12$
		$n, 3/2$	0	0	0	$-30 \pm 14$
N(1700) $D_{13}$	${}^4 8_{3/2}[70, 1^-]$	$p, 1/2$	0	0	0	$-22 \pm 13$
		$n, 1/2$	+8	+11	+11	$0 \pm 56$
		$p, 3/2$	0	0	0	$0 \pm 19$
		$n, 3/2$	+43	+57	+57	$-2 \pm 44$
N(1710) $P_{11}$	${}^2 8_{1/2}[70, 0^+]$	$p, 1/2$	-52	-27	-22	$+5 \pm 16$
		$n, 1/2$	+17	+9	+7	$-5 \pm 23$
N(1720) $P_{13}$	${}^2 8_{3/2}[56, 2^+]$	$p, 1/2$	+151	+119	+118	$+52 \pm 39$
		$n, 1/2$	-43	-34	-33	$-2 \pm 26$
		$p, 3/2$	-50	-39	-39	$-35 \pm 24$
		$n, 3/2$	0	0	0	$-43 \pm 94$
N(1990) $F_{17}$	${}^4 8_{7/2}[70, 2^+]$	$p, 1/2$	0	0	0	$+24 \pm 30$
		$n, 1/2$	+9	+22	+23	$-49 \pm 45$
		$p, 3/2$	0	0	0	$+31 \pm 55$
		$n, 3/2$	+12	+28	+29	$-122 \pm 55$

<sup>a</sup> The results in this line are obtained by introducing a mixing angle as in Eq. (10.3).

Table XI: Same as Table X, but for delta resonances.

Resonance	State	$\mu$	$A_{\mu}^{p,n}(\text{th})$			$A_{\mu}^{p,n}(\text{exp})$
			(1)	(2)	(3)	
$\Delta(1232)P_{33}$	${}^4 10_{3/2}[56, 0^+]$	1/2	-90	-91	-91	$-141 \pm 5$
		3/2	-155	-158	-157	$-258 \pm 12$
$\Delta(1600)P_{33}$	${}^4 10_{3/2}[56, 0^+]$	1/2	-37	-7	+0	$-20 \pm 29$
		3/2	-64	-12	+0	$+1 \pm 22$
$\Delta(1620)S_{31}$	${}^2 10_{1/2}[70, 1^-]$	1/2	-44	-51	-51	$+19 \pm 16$
						$+30 \pm 10$
$\Delta(1700)D_{33}$	${}^2 10_{3/2}[70, 1^-]$	1/2	-62	-82	-82	$+116 \pm 17$
		3/2	-62	-83	-82	$+77 \pm 28$
$\Delta(1900)S_{31}$	${}^2 10_{1/2}[70, 1^-]$	1/2	-2	-1	+0	$+10 \pm ?$
$\Delta(1905)F_{35}$	${}^4 10_{5/2}[56, 2^+]$	1/2	-10	-12	-11	$+27 \pm 13$
		3/2	-41	-49	-49	$-47 \pm 19$
$\Delta(1910)P_{31}$	${}^4 10_{1/2}[56, 2^+]$	1/2	+15	+18	+17	$-12 \pm 30$
$\Delta(1920)P_{33}$	${}^4 10_{3/2}[56, 2^+]$	1/2	-14	-18	-17	$+40 \pm ?$
		3/2	+25	+31	+30	$+23 \pm ?$
$\Delta(1930)D_{35}$	${}^2 10_{5/2}[70, 2^-]$	1/2	0	0	0	$-30 \pm 40$
		3/2	0	0	0	$-10 \pm 35$
$\Delta(1950)F_{37}$	${}^4 10_{7/2}[56, 2^+]$	1/2	+21	+29	+28	$-73 \pm 14$
		3/2	+27	+37	+36	$-90 \pm 13$

Figure 1: Collective model of baryons and its idealized string configuration (the charge distribution of the proton is shown as an example).

Figure 2: Schematic representation of the spectrum of the harmonic oscillator quark model with three identical constituents. The excitations are labeled by  $n = n_\rho + n_\lambda$  and  $L_t^\pi$ , where  $\pi$  denotes the parity and  $t$  the transformation property under  $S_3$  (the equivalent label of  $D_3$  is used). Each  $E$  state is doubly degenerate.

Figure 3: Vibrations of the string-like configuration of Figure 1.

Figure 4: Schematic representation of the vibrational and rotational excitations of the string-like configuration of Figure 1 with three identical constituent parts. The vibrational excitations are labeled by  $(n_u, n_v + n_w)$  and the rotational levels by  $K, L_t^\pi$ , where  $K$  is the projection of the angular momentum  $L$ ,  $\pi$  denotes the parity and  $t$  the overall (vibrational plus rotational) transformation property under the point group  $D_3$ . Each  $E$  state is doubly degenerate.

Figure 5: Plot of  $M^2$  versus  $L$  for a selected number of nucleon resonances. The lines represent the fit with  $\alpha = 1.064 \text{ GeV}^2$ .

Figure 6: Mass spectrum of some nucleon resonances. Solid lines: collective string model, Eq. (6.1). Dotted lines: relativized quark model [5]. Circles and vertical lines: experimental masses and their uncertainties, taken from [21].

Figure 7: Comparison between the experimental proton electric form factor  $G_E^p$  and the calculations with  $R^2 = 0$  (harmonic oscillator, dotted line),  $R^2 = 0.5$  and  $1.0$  (distributed string, dashed and solid line). The experimental data, taken from a compilation in [37], and the calculations are divided by the dipole form factor,  $F_D = 1/(1 + Q^2/0.71)^2$ .

Figure 8: Comparison between the experimental magnetic transition form factor for  $\Delta(1232)P_{33}$  and the calculations with  $R^2 = 0$  (harmonic oscillator, dotted line),  $R^2 = 0.5$  and  $1.0$  (distributed string, dashed and solid line). The experimental data, taken from the compilation in [23], and the calculations are divided by  $3F_D$ .

Figure 9: Comparison between the experimental transition form factor for the  $N(1520)D_{13}$  resonance and the calculations with  $R^2 = 0$  (harmonic oscillator, dotted line) and  $R^2 = 1.0$  (distributed string, solid line). The experimental data are taken from the compilation in [38].

Figure 10: Same as Figure 9, but for the  $N(1535)S_{11}$  resonance. Two calculations are shown, one with no mixing  $\theta = 0^\circ$ , and one with a mixing angle  $\theta = -38^\circ$  (see Eq. (10.3)). The experimental data are taken from the compilation in [23].

Figure 11: Same Figure 10, but for the  $N(1650)S_{11}$  resonance. The experimental data are taken from the compilation in [23].

Figure 12: Same as Figure 9, but for the  $N(1680)F_{15}$  resonance. The experimental data are taken from the compilation in [38].

Figure 13: Comparison between the experimental proton helicity asymmetry for the  $N(1520)D_{13}$  resonance and the calculations with  $R^2 = 0$  (harmonic oscillator, dotted line) and  $R^2 = 1.0$  (distributed string, solid line). The experimental data are taken from the compilation in [23].

Figure 14: Same as Figure 13, but for the  $N(1680)F_{15}$  resonance. The experimental data are taken from the compilation in [23].

Figure 15: Geometric intrinsic variables characterizing the shape of baryons.



Figure 2

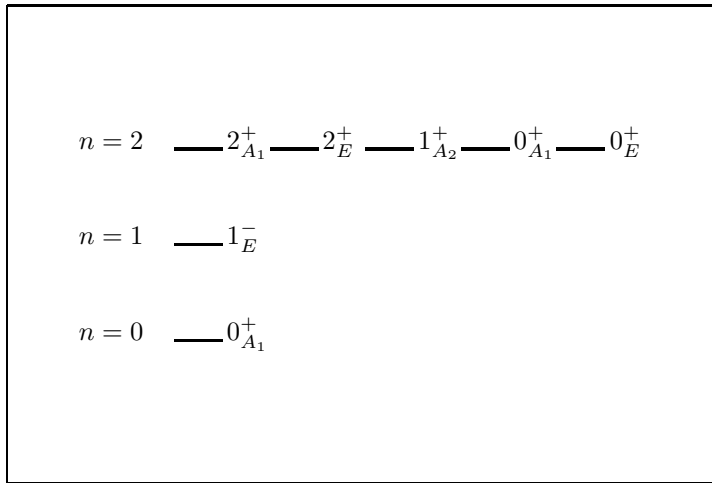


Figure 3

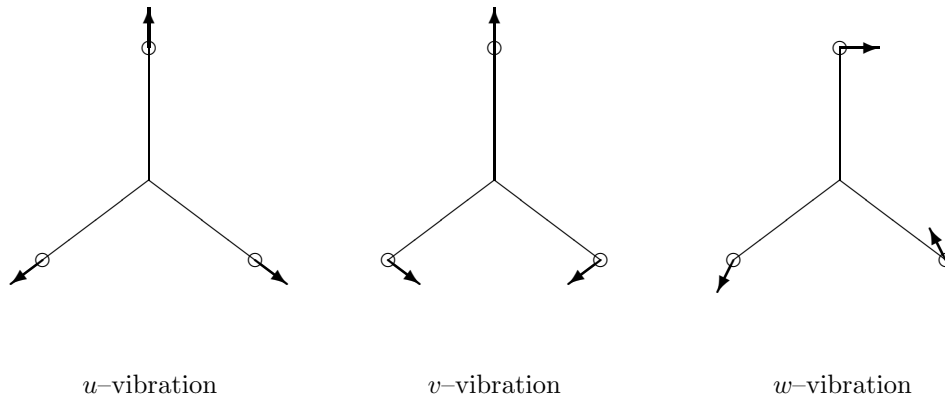


Figure 4

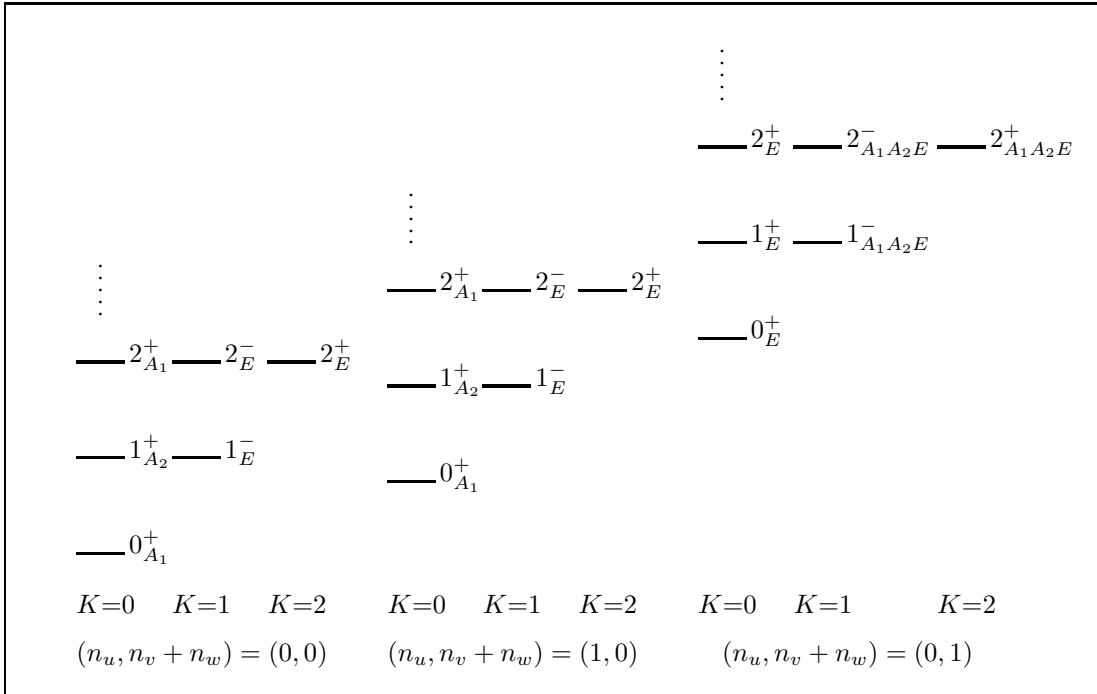
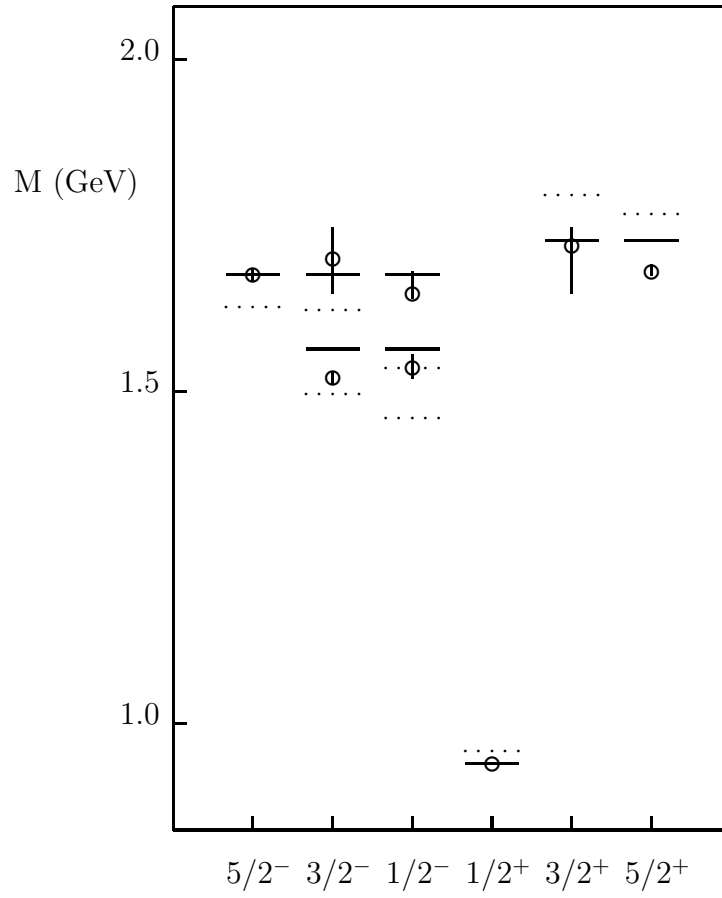


Figure 6



This figure "fig1-1.png" is available in "png" format from:

<http://arxiv.org/ps/nucl-th/9402012v1>

This figure "fig2-1.png" is available in "png" format from:

<http://arxiv.org/ps/nucl-th/9402012v1>

This figure "fig1-2.png" is available in "png" format from:

<http://arxiv.org/ps/nucl-th/9402012v1>

This figure "fig2-2.png" is available in "png" format from:

<http://arxiv.org/ps/nucl-th/9402012v1>



This figure "fig1-3.png" is available in "png" format from:

<http://arxiv.org/ps/nucl-th/9402012v1>

This figure "fig2-3.png" is available in "png" format from:

<http://arxiv.org/ps/nucl-th/9402012v1>

This figure "fig1-4.png" is available in "png" format from:

<http://arxiv.org/ps/nucl-th/9402012v1>

This figure "fig2-4.png" is available in "png" format from:

<http://arxiv.org/ps/nucl-th/9402012v1>

This figure "fig1-5.png" is available in "png" format from:

<http://arxiv.org/ps/nucl-th/9402012v1>

This figure "fig2-5.png" is available in "png" format from:

<http://arxiv.org/ps/nucl-th/9402012v1>

This figure "fig2-6.png" is available in "png" format from:

<http://arxiv.org/ps/nucl-th/9402012v1>